



## Long-term Atmospheric Deposition of Nitrogen and Sulfur and Assessment of Critical Loads Exceedances at Canadian Rural Locations

Irene Cheng<sup>1</sup>, Leiming Zhang<sup>1</sup>, Zhusansi He<sup>1</sup>, Hazel Cathcart<sup>1</sup>, Daniel Houle<sup>2</sup>, Amanda Cole<sup>1</sup>, Jian Feng<sup>1</sup>, Jason O'Brien<sup>1</sup>, Anne Marie Macdonald<sup>1</sup>, Julian Aherne<sup>3</sup> and Jeffrey Brook<sup>4</sup>

<sup>1</sup>Air Quality Research Division, Atmospheric Science and Technology Directorate, Science and Technology Branch, Environment and Climate Change Canada, Toronto, Ontario, M3H 5T4, Canada

<sup>2</sup>Aquatic Contaminants Research Division, Water Science and Technology Directorate, Science and Technology Branch, Environment and Climate Change Canada, Montréal, Quebec, H2Y 2E7, Canada

<sup>3</sup>School of Environment, Trent University, Peterborough, Ontario, K9L 0G2, Canada

<sup>4</sup>Dalla Lana School of Public Health and Department of Chemical Engineering and Applied Chemistry, University of Toronto, Toronto, Ontario, M5T 3M7, Canada

Correspondence to: Leiming Zhang ([leiming.zhang@ec.gc.ca](mailto:leiming.zhang@ec.gc.ca)) and Irene Cheng ([irene.cheng@ec.gc.ca](mailto:irene.cheng@ec.gc.ca))

**Abstract.** Daily air concentrations of inorganic nitrogen (N) species, including gaseous  $\text{HNO}_3$  and particulate-bound (p) $\text{NH}_4^+$  and p $\text{NO}_3^-$ , and sulfur (S) species, including  $\text{SO}_2$  and p $\text{SO}_4^{2-}$ , and precipitation concentrations of  $\text{NO}_3^-$ ,  $\text{NH}_4^+$  and  $\text{SO}_4^{2-}$ , have been routinely monitored by the Canadian Air and Precipitation Monitoring Network (CAPMoN) since 1983. Data at 15 rural sites from 2000-2018 were used to estimate dry and wet N and S deposition fluxes, which were then used to explore their spatiotemporal trends and assess ecosystem damage through a retrospective analysis of critical loads (CL) exceedances. Total (dry+wet) N deposition ranged from 1.7-9.5 kg N  $\text{ha}^{-1}$   $\text{yr}^{-1}$  among the 15 sites, though dry deposition of  $\text{NH}_3$  and some oxidized N species were not included due to a lack of data. Based on additional N measurements in 2010 at one of the sites, annual total N deposition may be underestimated by up to 32%. Total N deposition was dominated by wet  $\text{NO}_3^-$  and wet  $\text{NH}_4^+$  deposition, which together comprised 71-95%. Contributions to dry N deposition were 40-74% by  $\text{HNO}_3$ , 11-40% by p $\text{NH}_4^+$  and 5-25% by p $\text{NO}_3^-$ . Total S deposition ranged from 1.3-8.5 kg S  $\text{ha}^{-1}$   $\text{yr}^{-1}$  and was dominated by wet deposition of  $\text{SO}_4^{2-}$  and dry deposition of  $\text{SO}_2$ . Relative percentages of wet and dry S deposition were 45-89% and 11-55%, respectively. Acidic ion fluxes were greatest in southeastern Canada and were comparable among the west coast, prairie, remote and eastern Canadian sites. Oxidized N (dry  $\text{HNO}_3$ , dry p $\text{NO}_3^-$ , wet  $\text{NO}_3^-$ ) deposition was greater than that of reduced N (dry p $\text{NH}_4^+$ , wet  $\text{NH}_4^+$ ) in the early 2000s. In 2014-2018, reduced N deposition surpassed that of oxidized N in southeastern Canada. Total N and S deposition decreased significantly at a rate of -0.03 to -0.25 kg N  $\text{ha}^{-1}$   $\text{yr}^{-1}$  (-1.1% to -3.3%  $\text{yr}^{-1}$ ) and -0.08 to -0.66 kg S  $\text{ha}^{-1}$   $\text{yr}^{-1}$  (-3.5% to -6.6%  $\text{yr}^{-1}$ ), respectively, among the sites. The weak declining trend in total N deposition at the west coast site was consistent with the slower decline in  $\text{NO}_x$  emissions in western Canada. Reductions in total N deposition were driven by its oxidized form as trends in reduced N were non-significant. As a result, reduced N contributions to total N deposition increased on average from 42% in 2000-2004 to 53% in 2014-2018. Anthropogenic  $\text{NO}_x$  and  $\text{SO}_2$  emissions reductions in both eastern Canada and eastern U.S. were highly effective in reducing



total oxidized N and total S deposition, respectively, in eastern Canada. Acidic deposition exceeded terrestrial CL at 5 of the  
35 14 sites and aquatic CL at 2 of the 5 sites in the early 2000s. However, exceedances have been trending downwards and acidic deposition fluxes were mostly near or below CL after 2012 for the subset of sites assessed, which support recovery from historical acidification. Further assessments of CL exceedances are required in other Canadian regions susceptible to acidification and affected by elevated or increasing N and S emissions.

## 1 Introduction

40 Nitrogen (N) and sulfur (S) are the major chemical constituents of acidic deposition. Long-term atmospheric inputs of N and S contribute to acidification of terrestrial and aquatic ecosystems as well as eutrophication in the case of N. It is well established that acidic deposition results in the degradation of soil and water quality leading to detrimental effects on vegetation, forests and aquatic and terrestrial wildlife (Driscoll et al., 2001; ECCC, 2004; Bergström and Jansson, 2006; Pardo et al., 2011; Wright et al., 2018). Further, recovery from acidification effects can take decades even as acidifying  
45 deposition decreases (Shao et al., 2020).

Atmospheric deposition of N and S occurs via both wet and dry deposition. Wet deposition of ammonium ( $\text{NH}_4^+$ ), nitrate ( $\text{NO}_3^-$ ) and sulfate ( $\text{SO}_4^{2-}$ ) are routinely monitored around the world. A review of global acidic deposition measurements up to 2005-2007 identified eastern North America as one of the regions having the highest wet deposition fluxes of N and S  
50 (Vet et al., 2014). Since policies were introduced to reduce anthropogenic  $\text{NO}_x$  and  $\text{SO}_2$  emissions (dominant precursors of N and S deposition), wet deposition of  $\text{NO}_3^-$  and  $\text{SO}_4^{2-}$  have declined significantly in Canada and the U.S. (Du et al., 2014; Sickles and Shadwick, 2015; Li et al., 2016; Cheng and Zhang, 2017; Zhang et al., 2018; Feng et al., 2021; Burns et al., 2021; Likens et al., 2021). The rate of decline in eastern North America was 1.6-2.0% and 2.5-2.9% per year for  $\text{NO}_3^-$  and  $\text{SO}_4^{2-}$  wet deposition, respectively between 1989 and 2016 (Feng et al., 2021). Wet  $\text{NH}_4^+$  deposition was relatively  
55 unchanged in Canada (Cheng and Zhang, 2017; Feng et al., 2021) and in most regions of the U.S. (Lehmann et al., 2007; Du et al., 2014; Li et al., 2016; Feng et al., 2021) between the 1990s and 2015. A slight increasing trend was found in the U.S. Midwest, which appears to coincide with increasing ammonia ( $\text{NH}_3$ ) emissions contributing to particulate ammonium ( $\text{pNH}_4^+$ ; Du et al., 2014; Li et al., 2016).

60 Unlike wet deposition, long-term data on dry deposition of N and S are sparse because of the challenges in accurately measuring dry deposition fluxes. Dry deposition fluxes are typically estimated using the inferential method, which is based on the observed or modeled surface concentrations and modeled dry deposition velocities of N and S compounds (Fowler et al., 2005; Holland et al., 2005; Zhang et al., 2003, 2009; Flechard et al., 2011; Schwede et al., 2011; Staelens et al., 2012). Particulate sulfate ( $\text{pSO}_4^{2-}$ ) and  $\text{SO}_2$  are the main constituents of dry S deposition. Dry deposition of N comprises oxidized  
65 (e.g.,  $\text{pNO}_3^-$ ,  $\text{HNO}_3$ ,  $\text{NO}_2$ ,  $\text{HONO}$ ,  $\text{N}_2\text{O}_5$ , peroxy nitrates) and reduced (e.g.,  $\text{pNH}_4^+$ ,  $\text{NH}_3$ ) species and organic N (Walker et



al., 2020). Most estimates of dry N deposition include  $\text{pNO}_3^-$ ,  $\text{HNO}_3$ ,  $\text{pNH}_4^+$  and/or  $\text{NH}_3$  given that their ambient air concentrations are routinely monitored or modeled.

Dry deposition makes up a significant proportion of the total deposition. Approximately 28-75% of total N deposition in the 70 continental U.S. (Li et al., 2016; Zhang et al., 2018; Walker et al., 2019; 2020; Benish et al., 2022), 10-50% of total N deposition, 24-46% of total S deposition in Canada (ECCC, 2004; Zhang et al., 2009), and 50-52% of total N deposition in China (Pan et al., 2012; Xu et al., 2015) have been attributed to dry deposition. Reduced  $\text{N}$  is playing an increasingly important role in dry deposition owing both to agricultural and wildfire emissions of  $\text{NH}_3$  and also to emissions reductions in  $\text{NO}_x$  (Pan et al., 2012; Xu et al., 2015; Butler et al., 2016; Li et al., 2016; Kharol et al., 2018; Zhang et al., 2018; McHale et 75 al., 2021). Nevertheless, oxidized N deposition continued to dominate over reduced N or exhibit increasing trends in some regions (Zhang et al., 2009; Liu et al., 2013; Kharol et al., 2018). There are a few studies tracking the long-term trends in both dry and wet deposition of N and S (Fowler et al., 2005; Sickles and Shadwick, 2015; Li et al., 2016; Zhang et al., 2018; Nopmongcol et al., 2019; Yu et al., 2019; Tan et al., 2020; Wen et al., 2020; Benish et al., 2022), which provides a more 80 complete assessment of the acidic deposition budget. Previous studies demonstrate that dry deposition cannot be neglected when assessing the effects of anthropogenic emissions reductions on acidic deposition. Total (dry+wet) deposition of N and S are also necessary for evaluating exceedances of critical loads (threshold values for acidic deposition that can be tolerated by ecosystems; Nilsson and Grennfelt, 1988) and potential negative effects on ecosystems (e.g., Ellis et al., 2013; Zhao et al., 2017; Makar et al., 2018).

85 The Canadian Air and Precipitation Monitoring Network (CAPMoN) measures inorganic N and S among other pollutants in air and precipitation at rural and remote locations across Canada (ECCC, 2017). Previous analyses of CAPMoN data largely focused on long-term trends in N and S in ambient air or in wet deposition (ECCC, 2004; Zbieranowski and Aherne, 2011; Vet et al., 2014; Cheng and Zhang, 2017; Feng et al., 2021). Dry deposition of N species were also estimated at CAPMoN sites through a series of short term field campaigns in the early 2000s (Zhang et al., 2009). Hence, this study expands on the 90 scope of previous assessments by focusing on dry and total N and S deposition during the past two decades. The objectives were to: (1) estimate the long-term dry deposition fluxes of inorganic N and S at 15 CAPMoN sites using the inferential approach; (2) analyze the spatiotemporal trends in dry and total (dry+wet) deposition and in anthropogenic emissions; (3) examine the relative contributions from dry and wet deposition and from various N and S species; and (4) discuss the implications of the deposition results on Canadian ecosystems based on an analysis of critical loads exceedances.



## 95 2 Methodology

### 2.1 Measurements of air concentration of pollutants and wet concentration of inorganic ions

Atmospheric deposition of N and S at 15 CAPMoN sites were analyzed in this study. The sites were selected because of their long-term (8 to 19 years) data availability, which are suitable for temporal trend analyses. All sites are considered regionally representative, meaning that the influence of local pollution sources is minimal. The 15 sites consist of one site 100 on the west coast (SAT), one site in the prairies (BRA), two sites in the southeastern region (LON, EGB), four sites in the greater southeastern region (ALG, SPR, CHA, FRE) which are located at higher latitudes compared to LON and EGB, four remote inland sites (ELA, BON, CPS, LED) and three sites in the Atlantic region (KEJ, MIN, BAB). MIN is located in eastern Quebec, but is classified as part of the Atlantic region in this paper. A map of the sites is shown in Fig. 1 and site descriptions are provided in Table S1 of the Supplement.

105

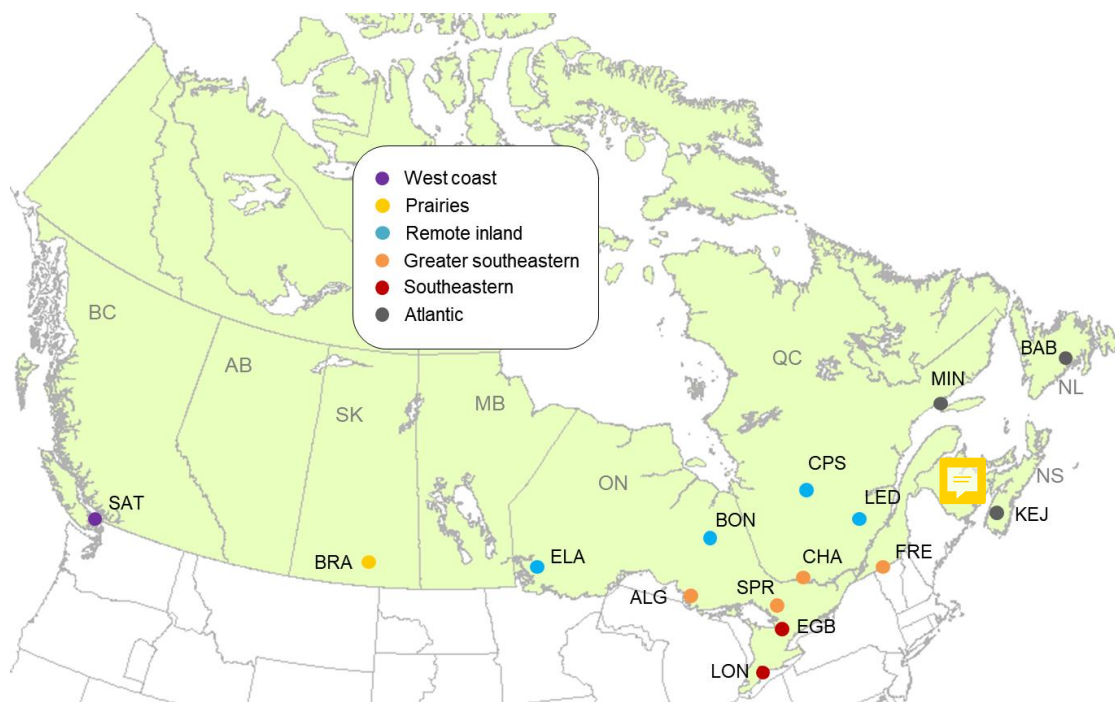


Figure 1: Map of CAPMoN sites analyzed in this study and their regional designations

Methods for sampling and analysis of air and precipitation have been described in previous studies (Sirois and Fricke, 1992; 110 Sirois et al., 2000). CAPMoN collects 24-h integrated air samples using an open-face three-stage filter. The non-size selective air filters are sent to the CAPMoN laboratory in Toronto, Canada, for chemical analysis including particulate sulfate ( $p\text{SO}_4^{2-}$ ), nitrate ( $p\text{NO}_3^-$ ) and ammonium ( $p\text{NH}_4^+$ ), gaseous  $\text{HNO}_3$  and  $\text{SO}_2$  (analyzed as dissolved  $\text{NO}_3^-$  and  $\text{SO}_4^{2-}$ ), calcium ( $\text{Ca}^{2+}$ ), magnesium ( $\text{Mg}^{2+}$ ), sodium ( $\text{Na}^+$ ), potassium ( $\text{K}^+$ ) and chloride ( $\text{Cl}^-$ ) ions. Non-sea salt  $p\text{SO}_4^{2-}$  was



approximated at coastal sites (i.e., SAT, KEJ, MIN and BAB) using the WMO method for estimating non-sea salt sulfate in  
115 precipitation (WMO, 2004). Precipitation is sampled over a 24-h collection period using a wet-only collector that opens  
when it senses rain or snow. Samples are sent to the CAPMoN laboratory for measurement of pH and major inorganic ions  
including total  $\text{SO}_4^{2-}$ ,  $\text{NO}_3^-$  and  $\text{NH}_4^+$  as well as  $\text{Ca}^{2+}$ ,  $\text{Mg}^{2+}$ ,  $\text{Na}^+$ ,  $\text{K}^+$  and  $\text{Cl}^-$  in precipitation. Rain and snow gauge  
measurements are used to calculate wet deposition fluxes. The CAPMoN sites and monitoring equipment are maintained  
regularly by field technicians and site operators. The data are quality controlled using the Research Data Management and  
120 Quality Assurance System (RDMQ) software (McMillan et al., 2000) and finalized by ECCC's National Atmospheric  
Chemistry (NAtChem) team. The CAPMoN air filter pack and precipitation chemistry datasets can be downloaded from the  
Government of Canada's Open Data Portal (ECCC, 2021b,c). Annual wet deposition fluxes of N and S species were  
calculated from their precipitation-weighted mean concentrations multiplied by the annual precipitation amount. Annual  
fluxes were reported only if data completeness thresholds were met. The criteria were that (a) at least 90% of the days in the  
125 year, and at least 60% of the days in each quarter, had a valid precipitation depth measurement, and (b) a valid concentration  
measurement was available for at least 70% of the annual precipitation and 60% in each quarter.

Additional N species including NO,  $\text{NO}_2$ , total reactive N ( $\text{NO}_y$ ) and  $\text{NH}_3$  have been measured at selected CAPMoN sites.  
Measurements at the EGB site in 2010 were analyzed in this study to estimate total N dry deposition after including the  
130 missing N species and examine the relative contributions of various N species to N dry deposition, following the approach  
described in Zhang et al. (2009). NO,  $\text{NO}_2$  and  $\text{NO}_y$  were measured at 1-min intervals using Thermo Electron Model 42C  
trace level gas analyzers. The analyzers measured NO based on the chemiluminescent reaction with ozone.  $\text{NO}_2$  was  
converted to NO using a Droplet Measurements BLC photolytic converter, while  $\text{NO}_y$  (NO,  $\text{NO}_2$ ,  $\text{HNO}_3$ ,  $\text{HO}_2$ ,  $\text{pNO}_3^-$ ,  $\text{N}_2\text{O}_5$ ,  
PAN, organic nitrates, and others) were converted to NO using a molybdenum converter heated to 325°C. Continuous  
135 measurements of  $\text{NH}_3$  were made using a modified Thermo 42C trace level chemiluminescence based analyzer. The  
measurement technique is based on the difference in responses of various N species converted to NO at elevated  
temperatures over stainless steel and molybdenum converters. The instrument was found to efficiently convert  $\text{NH}_3$  to NO at  
750°C over the stainless steel converter and inefficiently (<1%) over the molybdenum converter. In efforts to minimize any  
possible effects of ammonium nitrate volatilization, the sample inlet filter was changed daily. Automated instrument  
140 calibrations were performed every 25 hours, and the instruments were audited approximately every three months against a  
National Institute of Standards and Technology (NIST) standard. Mixing ratios of unknown  $\text{NO}_y$  were estimated by  
subtracting the measured  $\text{NO}_y$  species (NO,  $\text{NO}_2$ ,  $\text{HNO}_3$ ,  $\text{pNO}_3^-$ ) from total  $\text{NO}_y$ .

## 2.2 Dry deposition model

Dry deposition fluxes were estimated using the inferential method (observed surface concentration multiplied by the  
145 modeled dry deposition velocity ( $V_d$ )). Models for deriving  $V_d$  of gaseous compounds and  $\text{PM}_{2.5}$  and  $\text{PM}_{2.5-10}$  have been  
described in previous studies (Zhang et al., 2003; Zhang and He, 2014). Surface meteorological fields used in the  $V_d$



calculations were obtained from 19 years (2000-2018) of model reanalysis data (10 km resolution) from the Precipitation and Ground Surface Reanalysis (REQA) project (Gasset et al., 2021). Land use data and leaf area index (LAI) within a 3 km circle of each site (Table S1) were extracted from MODIS satellite data to compute land use area-weighted  $V_d$ 's. The same 150 models, meteorological data and land use data were recently used to produce a  $V_d$  database across North America, and more information regarding the model setup and data input can be found in Zhang et al. (2022).

In Eq. 1 to 4,  $V_d$  of  $pSO_4^{2-}$ ,  $pNO_3^-$  and  $pNH_4^+$  were determined using  $V_d$  of  $PM_{2.5}$  and  $PM_{2.5-10}$  and observed fine fractions of particulate inorganic ions (i.e.  $PM_{2.5}$ /total PM) following Zhang et al. (2008).  $V_d$  of unknown  $NO_y$  was estimated using Eq. 5 155 (Zhang et al., 2009).

$$V_d(pSO_4^{2-}) = 0.95*V_{d(PM2.5)} + 0.05*V_{d(PM2.5-10)}, \quad (1)$$

$$V_d(pNO_3^-, \text{Nov to Apr}) = 0.85*V_{d(PM2.5)} + 0.15*V_{d(PM2.5-10)}, \quad (2)$$

$$V_d(pNO_3^-, \text{May to Oct}) = 0.3*V_{d(PM2.5)} + 0.7*V_{d(PM2.5-10)}, \quad (3)$$

$$160 \quad V_d(pNH_4^+) = V_{d(PM2.5)}, \quad (4)$$

$$V_d(\text{unknown } NO_y) = 0.05*V_{d(HNO_3)} + 0.3*V_{d(pNO_3^-)} + 0.65*V_{d(PAN)}, \quad (5)$$

Spatial and temporal patterns in  $V_d$  of N and S species are detailed in Section S1, Fig. S1 and Fig. S2 of the Supplement. Modeled  $V_d$  of N and S species in Table S2 were comparable to those in a previous study at CAPMoN sites (Zhang et al., 165 2009) and a review of N fluxes (Walker et al., 2020). Differences in the parameterizations between dry deposition models result in uncertainties of a factor of 2 to 3 in modeled  $V_d$  of N and S species and in their dry fluxes (Flechard et al., 2011; Schwede et al., 2011). Thus, it is important to use a consistent model framework for long-term data, as was applied in this study.

### 2.3 Data analysis methods

170 Long-term trends in atmospheric deposition of N and S and precursor emissions were estimated using Theil-Sen's slopes, and the statistical significance of the slope was determined using the Mann-Kendall test (Carslaw and Ropkins, 2012). This is a non-parametric trends analysis method typically applied to environmental data (Du et al., 2014; Cheng and Zhang, 2017). Prior to estimating the long-term trends in deposition, seasonally-average yearly fluxes for the four seasons were decomposed by LOESS (locally estimated scatterplot smoothing) because of the strong seasonality in the deposition fluxes. 175 Deposition fluxes were also summarized for a six-month period during cold (November to April) and warm seasons (May to October). N and S deposition at the Canadian sites were compared with province- or state-level  $NO_x$ ,  $NH_3$  and  $SO_2$  emissions in Canada (ECCC, 2021a) and the U.S. (USEPA, 2021), respectively. Emissions were categorized by geographical region namely western Canada, eastern Canada, western U.S. and eastern U.S. Emissions in eastern Canada and eastern U.S. have a greater likelihood of affecting the sites in the southeastern and Atlantic regions, whereas emissions



180 in western Canada and western U.S. are more likely to influence the west coast and prairie sites based on back trajectory analyses of CAPMoN sites (ECCC, 2004; Zhang et al., 2008). Emissions in the provinces of British Columbia, Alberta and Saskatchewan are considered part of western Canada and those in Ontario and Quebec are part of eastern Canada. Western U.S. emissions include those from the following states: CA, CO, ID, MT, NV, OR, UT, WA and WY. Eastern U.S. emissions include those from the following states: IL, IN, KY, MD, MI, MN, MO, NC, NJ, NY, OH, PA, TN, VA, WI and  
185 WV.

## 2.4 Critical loads estimation for lakes and soil

To provide a view of potential changes in exceedances of critical loads (CL) of acidity, aquatic CL were estimated for 31 lakes surrounding five CAPMoN sites (ALG 5 lakes, ELA 5 lakes, LED 6 lakes, BAB 7 lakes, KEJ 8 lakes) using the Steady-State Water Chemistry (SSWC) model. The approach is described in detail elsewhere (Jeffries et al., 2010; Aherne and Jeffries, 2015). Briefly, in the SSWC model, lake CL is quantified by the pre-acidification base cation flux in its catchment minus the Acid Neutralizing Capacity ( $ANC_{limit}$ ), the threshold above which harmful effects on fish population are not observed (Jeffries et al., 2010; Aherne and Jeffries, 2015). The contribution of dissolved organic carbon (DOC) to acidic charges has been taken into account in calculating the  $ANC_{limit}$  using Eq. 6 (Jeffries et al., 2010). The pre-acidification base cation fluxes were estimated using present-day fluxes, which were derived from current base cation concentrations and  
195 spatially-interpolated runoff values. The “F-factor” was used to adjust the present-day base cation fluxes to account for long-term changes in acidic deposition (Brakke et al., 1990). Exceedance was estimated using the lake CL Steady-State method following the Canadian Acid Deposition Science Assessment (ECCC, 2004) and Jeffries et al. (2010) and the total S and N deposition fluxes at the CAPMoN sites (Eq. 7). Unlike S deposition, only a fraction of the N deposition is acidifying given its biological retention in the terrestrial portion of lake catchments. Equation 7 includes total N deposition, which  
200 assumes surrounding soils are N saturated and all N deposition contributes to acidity (ECCC, 2004; Jeffries et al., 2010). This assumption will result in higher CL exceedance and is a worst-case scenario.

$$ANC_{limit} = 10 + (10*2/3)*DOC \text{ (mg L}^{-1}\text{)}, \quad (6)$$

$$\text{Lake CL Exceedance} = \text{Total S deposition} + \text{Total N deposition} - CL \text{ (eq ha}^{-1} \text{ yr}^{-1}\text{)}, \quad (7)$$

205

The simple mass balance (SMB) model for estimating terrestrial CL (Sverdrup, 1990; Sverdrup and De Vries, 1994; Posch et al., 2015) was used to approximate soil CL at 14 of the 15 CAPMoN stations. The SMB model is a steady-state model that relies on several simplifying assumptions, primarily that the soil is a homogenous compartment and depth is limited to the root zone. Critical loads are defined as a function based on the maximum S-based CL ( $CL_{maxS}$ ), maximum N-based CL ( $CL_{maxN}$ ), and long-term N removal in the soil ( $CL_{minN}$ ). An approximate 10 km x 10 km area based on the GEM-MACH v2 model grid (Moran et al., 2018) was chosen to represent the terrestrial ecosystem surrounding the stations for cohesion with contemporary deposition maps. The BRA site was omitted from the soil CL estimations as the area is entirely  
210



agricultural (i.e. soils are not natural and receive anthropogenic N inputs through fertilizer application). Three more sites (EGB, LON, and FRE) were predominately agricultural but had some ( $\geq 8\%$ ) natural or semi-natural soils, which are the 215 focus of the SMB model. Required input data, such as the soil weathering rate, nutrient uptake, and critical ANC leaching, were estimated according to CLRTAP (2004) and mapped at 250 m resolution (details in Supplement Section S2). Soil CL within each grid were summarized using the 5<sup>th</sup> percentile (Posch et al., 1993) and exceedance was estimated along the CL function using total S and N deposition from the representative CAPMoN station.

### 3 Results and Discussion

#### 220 3.1 N and S concentrations and emissions trends

The highest concentrations of atmospheric S and N were observed at LON and EGB, which are the two southeastern sites closest to industrialized and populated areas in the U.S. and Canada (Fig. S3 Supplement). The next highest concentrations were observed at sites in the greater southeastern region of Canada (FRE, CHA, SPR, and ALG). Concentrations of N and S at the west coast (SAT) and prairie sites (BRA) were similar to those of the greater southeastern region, except for their 225 lower  $\text{pSO}_4^{2-}$  and  $\text{pNH}_4^+$  concentrations. The lowest concentrations were observed at remote sites (ELA, BON, CPS, LED) and in the Atlantic region (KEJ, MIN, BAB). The rank order of the stations from highest to lowest total S concentration was LON, EGB, FRE, CHA, SPR, BRA, SAT, ALG, KEJ, LED, ELA, CPS, BON, MIN, and BAB. Similarly, the rank order of stations for total N concentration was LON, EGB, FRE, BRA, SPR, ALG, CHA, SAT, ELA, KEJ, LED, CPS, BON, MIN, and BAB.

230

Annual trends in S and N concentrations during the 2000-2018 period varied across regions. The largest declines in the annual mean concentrations were observed at the two southeastern sites (Fig. S4). Despite having recorded the highest  $\text{SO}_2$  concentrations among CAPMoN stations every year since 1983, concentrations at LON and EGB were comparable to those in the greater southeastern region and at the west coast site in 2017-2018 and were only slightly higher than those of remote 235 sites. The second largest decrease in annual mean concentrations of S and N were observed in the greater southeastern region. At the west coast site, the decrease in annual  $\text{SO}_2$  and  $\text{HNO}_3$  concentrations was similar to those in the greater southeastern region, while slight decreases were observed in annual  $\text{pSO}_4^{2-}$ ,  $\text{pNH}_4^+$  and  $\text{pNO}_3^-$ . Weak declining trends in S and N were also observed at remote and Atlantic sites. No trend in the annual concentrations was found at the prairie site.

240 Trends in the annual mean concentrations at CAPMoN sites were strongly influenced by emissions of  $\text{SO}_2$  and  $\text{NO}_x$  as noted in previous studies (ECCC, 2004; Cheng and Zhang, 2017; Feng et al., 2020).  $\text{SO}_x$  emissions declined significantly between 2000 and 2018 in Ontario and Quebec (73% reduction) as well as in the eastern U.S (90% reduction; Fig. S5a). Declines in both domestic emissions and transboundary pollution were the main factors driving the decrease in atmospheric S concentrations in southeastern Canada. Decreases in  $\text{SO}_x$  emissions in Ontario and Quebec were attributed to the ore and



245 minerals and electric power generation sectors, while the decrease in  $\text{SO}_2$  emissions in the eastern U.S. was predominantly from electric utilities (Fig. S5a). Decreasing trends in  $\text{NO}_x$  emissions drove the decrease in atmospheric N at LON and EGB and the decrease in  $\text{HNO}_3$  concentrations in the greater southeastern region.  $\text{NO}_x$  emissions in Ontario and Quebec decreased by ~55% from 2000-2015 as a result of emissions reductions from the transportation sector and began to level off from 2015-2018. In the eastern U.S., the percentage decrease from 2000 to 2018 was 66% for total  $\text{NO}_x$  emissions and 71%  
250 for transportation and electric utility  $\text{NO}_x$  emissions.  $\text{NH}_3$  emissions in Ontario and Quebec declined from 2002-2008 and were constant from 2008-2018. In the eastern U.S., there was a period of steady  $\text{NH}_3$  emissions from 2002-2011 (Fig. S5a), which was followed by a sharp drop from 2011-2014 and then an increase from 2014-2018 but emission levels were still below 2011 levels. Trends in  $\text{NH}_3$  emissions were primarily driven by agriculture activities (ECCC, 2021a; USEPA, 2021).

255 Weaker trends in atmospheric S and N at the west coast and prairie locations reflected the emission trends and levels in western Canada and the western U.S. Compared with Ontario and Quebec,  $\text{SO}_x$  and  $\text{NO}_x$  emissions reductions in the western provinces of Canada were relatively modest during the 2000-2018 period (Fig. S5b). This was also the case when western and eastern U.S. emissions were compared. Emission levels of  $\text{SO}_2$  and  $\text{NO}_x$  in the western U.S. were significantly lower than those of the eastern U.S. The lack of trend in atmospheric S and N at the prairie site was consistent with the  
260 leveling off in emissions of  $\text{SO}_x$  and  $\text{NO}_x$  in Saskatchewan where the prairie site is located. It is important to note that  $\text{NH}_3$  emissions have been rising since 2010 in western Canada (notably in Saskatchewan) and in the western U.S (Fig. S5b), which contrasts with the declining trend in eastern regions. The rise in  $\text{NH}_3$  emissions may have contributed to the secondary formation of  $\text{pNO}_3^-$  and  $\text{pNH}_4^+$ , which resulted in a weakened decreasing trend in  $\text{pNO}_3^-$  and  $\text{pNH}_4^+$  caused by declining  $\text{SO}_x$  and  $\text{NO}_x$  emissions.  $\text{SO}_2$  and  $\text{NO}_x$  emissions in North Dakota, U.S., which borders Saskatchewan to the south,  
265 have seen a dramatic increase between the early 2000s and 2014-2018 due to the Bakken oil and gas development (USEPA, 2021). Ongoing monitoring is required to assess the impact of these industrial activities on ambient N and S in Saskatchewan.

### 3.2 Dry deposition fluxes

#### 270 3.2.1 Geographical distribution

Dry deposition fluxes for each of the 15 sites were calculated for the period from 2000-2018. Table 1 presents a regional breakdown of annual dry deposition of S and N, averaged over the period, for the sites in each geographical area. For all 15 sites, the mean dry deposition was  $0.6 \text{ kg N ha}^{-1} \text{ yr}^{-1}$  and  $0.9 \text{ kg S ha}^{-1} \text{ yr}^{-1}$  (non-sea salt), where N ranged from 0.1 (MIN) to 1.9 (LON)  $\text{kg N ha}^{-1} \text{ yr}^{-1}$ , and S ranged from 0.2 (MIN) to 3.5 (LON)  $\text{kg S ha}^{-1} \text{ yr}^{-1}$  (Table 1 and Table S3). The values at  
275 MIN were particularly low in part because measurements began in 2009, after significant emission declines across the region. On a regional scale, the highest N and S dry deposition were observed at two sites in southeastern Canada (LON and



EGB), which are strongly affected by large urban sources and transboundary pollution. The lowest N and S dry deposition fluxes were observed at several remote sites (ELA, BON, CPS, LED) and in the Atlantic region (KEJ, MIN, BAB).

280 **Table 1: Regional breakdown of annual mean dry deposition fluxes of N and S (kg N or S ha<sup>-1</sup> yr<sup>-1</sup>) across Canada for the 2000-2018 period. Site ID and flux range in parentheses.**

	$\Sigma N$	$\Sigma S$	$HNO_3$	$pNO_3^-$	$pNH_4^+$	$SO_2$	$pSO_4^{2-}$
All sites	0.6 (0.1-1.9)	0.9 (0.2-3.5)	0.3 (0.05-0.8)	0.09 (0.01-0.4)	0.2 (0.05-0.7)	0.7 (0.1-3.0)	0.2 (0.1-0.6)
Southeastern (LON, EGB)	1.6 (1.4-1.9)	2.8 (2.0-3.5)	0.7 (0.6-0.8)	0.35 (0.3-0.4)	0.6 (0.5-0.7)	2.3 (1.6-3.0)	0.5 (0.4-0.6)
Greater southeastern (SPR, ALG, CHA, FRE)	0.5 (0.4-0.6)	0.64 (0.6-0.8)	0.3 (0.2-0.4)	0.05 (0.03-0.08)	0.13 (0.1-0.2)	0.5 (0.3-0.6)	0.15 (0.1-0.2)
West coast & prairie (SAT, BRA)	0.72 (0.71-0.74)	1.2 (1.0-1.4)	0.4 (0.3-0.6)	0.13 (0.1-0.2)	0.15 (0.1-0.2)	1.0 (0.8-1.3)	0.16 (0.1-0.2)
Atlantic (KEJ, MIN, BAB)	0.2 (0.1-0.3)	0.3 (0.2-0.5)	0.1 (0.05-0.2)	0.04 (0.03-0.04)	0.06 (0.05-0.1)	0.2 (0.1-0.3)	0.13 (0.1-0.2)
Remote continental (ELA, BON, CPS, LED)	0.2 (0.1-0.3)	0.3 (0.2-0.4)	0.1 (0.08-0.2)	0.02 (0.01-0.05)	0.07 (0.05-0.1)	0.17 (0.1-0.2)	0.1 (0.08-0.12)

Dry deposition fluxes for the regionally-grouped sites were compared over an early and recent 5-year period (i.e. 2000-2004 and 2014-2018). The spatial patterns in dry deposition of N and S remained consistent with the highest fluxes at the two 285 southeastern sites (Fig. 2). The major difference between the two periods was the large decrease in dry deposition fluxes at all sites. Dry deposition of N decreased by ~50%, while dry deposition of S decreased by ~71% from 2000-2004 to 2014-2018 (Table 2). This is similar in magnitude to  $SO_2$  and  $NO_x$  emissions reductions as discussed in section 3.1. Dry deposition of S on a mass basis was higher than that of N during 2000-2004; however, the fluxes of N and S were almost equivalent in the recent period (Fig. 2).

290

**Table 2: Percentage reduction in dry, wet and total (dry+wet) N and S deposition from 2000-2004 to 2014-2018 period. NA: not available due to incomplete data coverage. % reduction = (mean annual flux<sub>2000-2004</sub> - mean annual flux<sub>2014-2018</sub>)/mean annual flux<sub>2000-2004</sub>**

Site ID	Dry N	Dry S	Wet N	Wet S	Total N	Total S
SAT	39%	68%	18%	51%	24%	61%
BRA	NA	NA	NA	NA	NA	NA



ELA	39%	65%	17%	51%	19%	54%
ALG	56%	68%	32%	55%	33%	56%
BON	NA	NA	NA	NA	NA	NA
LON	55%	81%	25%	63%	32%	71%
EGB	51%	80%	15%	63%	23%	70%
SPR	58%	77%	22%	58%	26%	62%
CHA	58%	70%	35%	67%	37%	67%
CPS	46%	58%	36%	60%	37%	60%
FRE	51%	68%	26%	60%	28%	61%
LED	54%	65%	27%	53%	30%	55%
KEJ	66%	83%	29%	60%	34%	65%
MIN	NA	NA	NA	NA	NA	NA
BAB	NA	NA	NA	NA	NA	NA

295 The relative dry deposition of routinely-measured species was examined. Over the entire period (2000-2018),  $\text{HNO}_3$  contributions to dry deposition of N were greater than those of  $\text{pNO}_3^-$  and  $\text{pNH}_4^+$  at all sites ( $1.4\text{-}1.9 \text{ kg N ha}^{-1} \text{ yr}^{-1}$ ) (Table 1). This is because the dry deposition velocity of gaseous  $\text{HNO}_3$  is greater than that of particle N species (Table S2). The highest mean  $\text{HNO}_3$  dry deposition was observed in southeastern Canada, but in the greater southeastern region (less affected by urban regional transport) dry deposition was lower than at the west coast and prairie sites. Fluxes of  $\text{HNO}_3$  in the Atlantic region and remote sites ( $0.05\text{-}0.1 \text{ kg N ha}^{-1} \text{ yr}^{-1}$ ) were among the lowest in Canada. Overall, there were minor contributions of  $\text{pNH}_4^+$  and  $\text{pNO}_3^-$  to N dry deposition across Canada with the exception of two sites in southeastern Canada (Table 1). As for the spatial patterns, the relative contributions of N species to dry N deposition was compared for the early and recent periods and the percentages remained constant between the two periods.  $\text{HNO}_3$  contributed the greatest to N dry deposition (40-74%), followed by  $\text{pNH}_4^+$  (11-40%) and  $\text{pNO}_3^-$  (5-25%) depending on the site (Fig. 2). The relative composition of N dry deposition varied from site to site yet remained relatively stable at each site during the two 5-year periods. The relative amounts of oxidized N dry deposition, which comprised  $\text{HNO}_3$  and  $\text{pNO}_3^-$ , were nearly equivalent in the two periods. This is because of decreases in the dry deposition of both  $\text{HNO}_3$  and  $\text{pNO}_3^-$  between the two periods (Fig. 2).

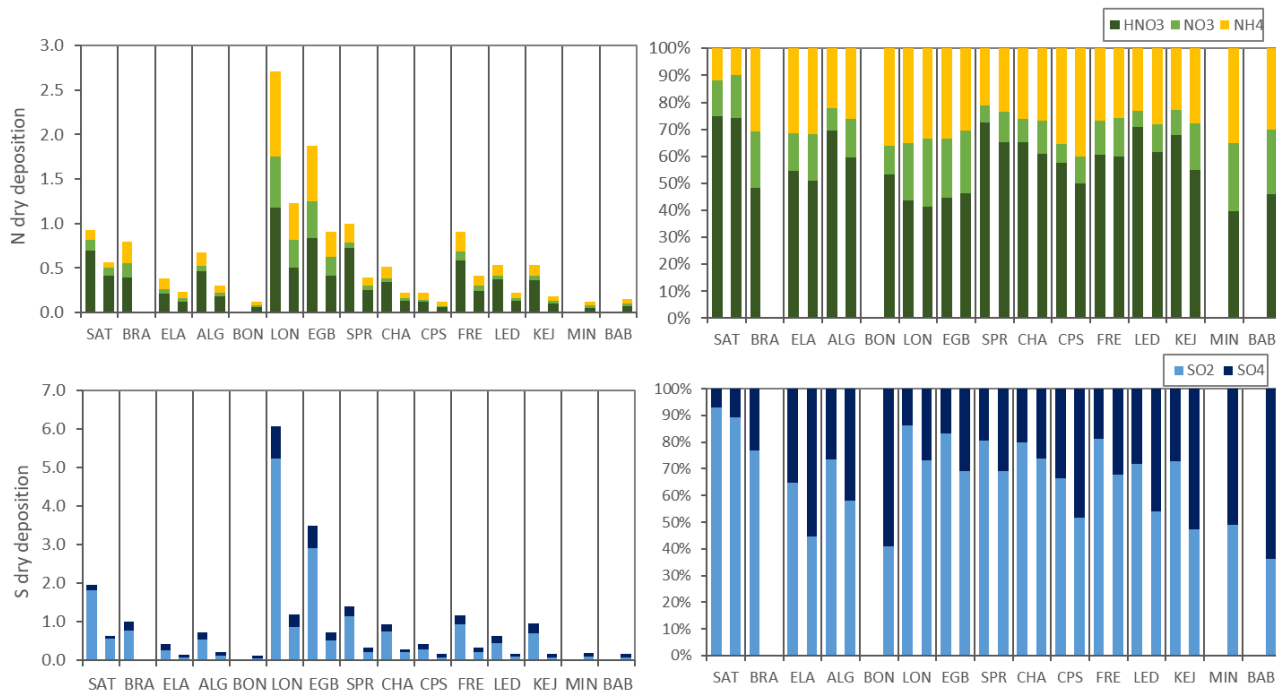


**Figure 2: Mean N and S dry deposition fluxes (kg N or S ha<sup>-1</sup> yr<sup>-1</sup>) and the percentage of N or S species in dry deposition during 2000-2004 (1<sup>st</sup> bar) and 2014-2018 (2<sup>nd</sup> bar)**

Gaseous NH<sub>3</sub>, NO<sub>2</sub>, PAN, PPN and other NO<sub>y</sub> can also contribute to N dry deposition. It was estimated that 50-65% of the N dry deposition during 2002-2005 at eight CAPMoN sites was attributed to N compounds that are not routinely-monitored by CAPMoN, while 35-50% was attributed to HNO<sub>3</sub>, pNO<sub>3</sub><sup>-</sup> and pNH<sub>4</sub><sup>+</sup> (Zhang et al., 2009). Based on additional N measurements at EGB in 2010, the relative dry deposition of routinely versus non-routinely monitored N species was 30% and 70%, respectively, on an annual basis. N dry deposition including those of routine species, NO<sub>2</sub>, NH<sub>3</sub> and unknown NO<sub>y</sub> (e.g., PAN, PPN, other N species) was 3.6 kg N ha<sup>-1</sup> in 2010 (Table 3). This was about three times the dry deposition of routine N species (1.1 kg N ha<sup>-1</sup> in 2010). Table 3 shows that the dominant species in N annual dry deposition were NH<sub>3</sub> (58%) and HNO<sub>3</sub> (15%) followed by pNH<sub>4</sub><sup>+</sup>, NO<sub>2</sub>, pNO<sub>3</sub><sup>-</sup> and unknown NO<sub>y</sub>, respectively. The N dry flux at EGB in 2010 was slightly lower than the 3.9 kg N ha<sup>-1</sup> estimated in 2002 (Zhang et al., 2009). Oxidized N was the dominant form of N dry deposition in 2002 (Zhang et al., 2009). In 2010, oxidized and reduced forms comprised 32% and 68%, respectively, of the N dry deposition. This change was driven by a decrease in ambient oxidized N (9.5 ppbv in 2002 to 3.4 ppbv in 2010) and an increase in ambient reduced N notably from NH<sub>3</sub> (1.2 ppbv in 2002 to 3.1 ppbv in 2010). It should be noted that NH<sub>3</sub> undergoes frequent bi-directional air-surface exchange processes in agricultural areas, and its dry deposition estimates at EGB presented here should be treated as upper-end values. Nevertheless, given NH<sub>3</sub> was by far the largest contributor to N



dry deposition for this one-year period at EGB, including  $\text{NH}_3$  in routine monitoring should be a priority in order to accurately assess the long-term levels and effects of N deposition.

At the 15 CAPMoN sites, dry deposition of S was dominated by  $\text{SO}_2$  at most sites except at BON, MIN and BAB, which had 330 equal contributions from  $\text{SO}_2$  and  $\text{pSO}_4^{2-}$  because of the relatively low  $\text{SO}_2$  concentrations at these three sites. Dry deposition of  $\text{SO}_2$  was 1.6 and 3.0  $\text{kg S ha}^{-1} \text{yr}^{-1}$  at the two sites in southeastern Canada, which represented the highest fluxes among the sites. Dry deposition of  $\text{SO}_2$  in the greater southeastern region was only ~20% of that observed at the two sites in southeastern Canada (Table 1). Dry fluxes of  $\text{SO}_2$  at the west coast and prairie sites ranged from 0.8 to 1.3  $\text{kg S ha}^{-1} \text{yr}^{-1}$ . The Atlantic region and remote sites recorded the lowest dry deposition of  $\text{SO}_2$  (0.1-0.3  $\text{kg S ha}^{-1} \text{yr}^{-1}$ ). Dry deposition fluxes 335 of non-sea salt  $\text{pSO}_4^{2-}$  were generally small at the majority of the sites except for the two sites in southeastern Canada (Table 1). This is because  $V_d$  of the particulate species are typically smaller than the gaseous compounds (Supplement Table S2). Concentrations of  $\text{pSO}_4^{2-}$  may be higher or lower than those of  $\text{SO}_2$  depending on the site (Fig. S3). The relative contribution of  $\text{SO}_2$  to S dry deposition generally decreased between the early and recent 5-year period (Fig. 2). In 2000-2004,  $\text{SO}_2$  contributed 65-93% of the S dry deposition depending on the site, while in the later period this ranged from 36-89%. The 340 relative dry deposition of  $\text{pSO}_4^{2-}$  increased over the years to 11-55% and exceeded that of  $\text{SO}_2$  at five sites in the 2014-2018 period (Fig. 2). Feng et al. (2020) showed that the relative fraction of  $\text{pSO}_4^{2-}$  to total S in ambient air rose by 50.6% as  $\text{SO}_2$  declined in the eastern U.S. and eastern Canada for the 1989-2016 period.

345 **Table 3: Breakdown of atmospheric deposition of non-routinely (NR) and routinely (R) monitored N species at the EGB site in 2010, on an annual basis and during cold (Jan-Apr, Nov-Dec) and warm (May-Oct) seasons**

		Flux ( $\text{kg N ha}^{-1} \text{yr}^{-1}$ )			Relative contributions to dry N deposition			Relative contributions to total N deposition		
		Annual	Cold	Warm	Annual	Cold	Warm	Annual	Cold	Warm
NR	Dry $\text{NO}_2$	0.3	0.3	0.3	8%	12%	7%	4%	6%	3%
NR	Dry $\text{NH}_3$	2.1	1.0	3.3	58%	43%	67%	27%	21%	33%
NR	Dry unknown $\text{NO}_y$	0.1	0.1	0.1	3%	4%	2%	1%	2%	1%
R	Dry $\text{HNO}_3$	0.6	0.4	0.7	15%	15%	15%	7%	7%	7%
R	Dry $\text{pNO}_3^-$	0.2	0.2	0.2	6%	10%	3%	3%	5%	2%
R	Dry $\text{pNH}_4^+$	0.3	0.4	0.3	9%	15%	6%	4%	7%	3%
R	Wet $\text{NO}_3^-$	1.7	1.3	1.9	-	-	-	21%	26%	19%
R	Wet $\text{NH}_4^+$	2.5	1.4	3.2	-	-	-	32%	27%	31%
NR+R	Oxidized N (dry, total)	1.2, 2.8	1.0, 2.3	1.3, 3.2	32%	41%	27%	36%	45%	32%
NR+R	Reduced N (dry, total)	2.5, 4.9	1.4, 2.8	3.6, 6.8	68%	59%	73%	64%	55%	68%
NR+R	Summed dry N	3.6	2.4	5.0						
NR+R	Total (dry+wet) N	7.8	5.1	10.0						



### 3.2.2 Seasonal patterns

Seasonal mean dry deposition of N and S are shown in Fig. 3. In the warm season (May to October), the deposition of HNO<sub>3</sub> was higher at most locations. For example, mean dry deposition of HNO<sub>3</sub> during the warm season was twice that of the cold season for the two sites in southeastern Canada and the prairie site (Fig. 3). This warm season increase is attributed to enhanced atmospheric oxidation especially at the more polluted sites, which are likely to observe higher oxidant mixing ratios. In the cold season (November to April), dry deposition of HNO<sub>3</sub> decreased while that of pNH<sub>4</sub><sup>+</sup> and pNO<sub>3</sub><sup>-</sup> increased slightly (Fig. 3). This is due to the temperature-dependent gas-particle partitioning process, which is conducive to the formation of ammonium nitrate in the cold season. The seasonal patterns in dry fluxes were consistent with those of the ambient air concentrations. Concentrations of HNO<sub>3</sub> were typically higher in the warm season, while pNO<sub>3</sub><sup>-</sup> were higher in the cold season (Feng et al., 2020).

Dry deposition of NH<sub>3</sub> at EGB in 2010 was higher in the warm season than the cold season. Seasonal fluxes in that year were comparable for NO<sub>2</sub> and unknown NO<sub>y</sub>. Further, relative contributions for the cold and warm season were 43% and 67% for NH<sub>3</sub>, 12% and 7% for NO<sub>2</sub>, and 4% and 2% for unknown NO<sub>y</sub> (Table 3). The higher NH<sub>3</sub> dry deposition in the warm season is due to the higher NH<sub>3</sub> mixing ratios resulting from elevated agricultural activity and their associated emissions and increased volatilization with warmer temperatures.

Unlike N, dry deposition of S was higher in the cold season, mainly driven by higher air concentrations of SO<sub>2</sub> (Fig. 3). On average, dry deposition of SO<sub>2</sub> in the cold season was ~0.25 kg S ha<sup>-1</sup> yr<sup>-1</sup> higher than that of the warm season, despite the somewhat lower cold season mean V<sub>d</sub> of SO<sub>2</sub> at most of the sites; however, this difference was as high ~1 kg S ha<sup>-1</sup> yr<sup>-1</sup> at SAT and LON. A likely explanation is that the atmospheric oxidation rate of SO<sub>2</sub> in the cold season is much lower, which resulted in the higher ambient SO<sub>2</sub> and its longer lifetime in the winter. This is consistent with model simulation results, which estimated that the lifetime of SO<sub>2</sub> during winter and summer were 48 h and 13 h, respectively (Lee et al., 2011). At the range of latitudes of the CAPMoN stations (~45–55°N), the average gas-phase SO<sub>2</sub> oxidation rate in the summer was approximately 11 times that of winter, with insignificant SO<sub>2</sub> conversion in the winter (Altshuller, 1979). Although the magnitude of the fluxes differed between seasons, the geographical distribution of the fluxes were generally consistent. In both seasons, S dry deposition was highest at the two sites in southeastern Canada followed by the west coast and prairie site. The Atlantic region and remote sites received the lowest dry deposition of S in the cold and warm seasons. For pSO<sub>4</sub><sup>2-</sup>, there were minor differences in the dry deposition fluxes between seasons (Fig. 3).



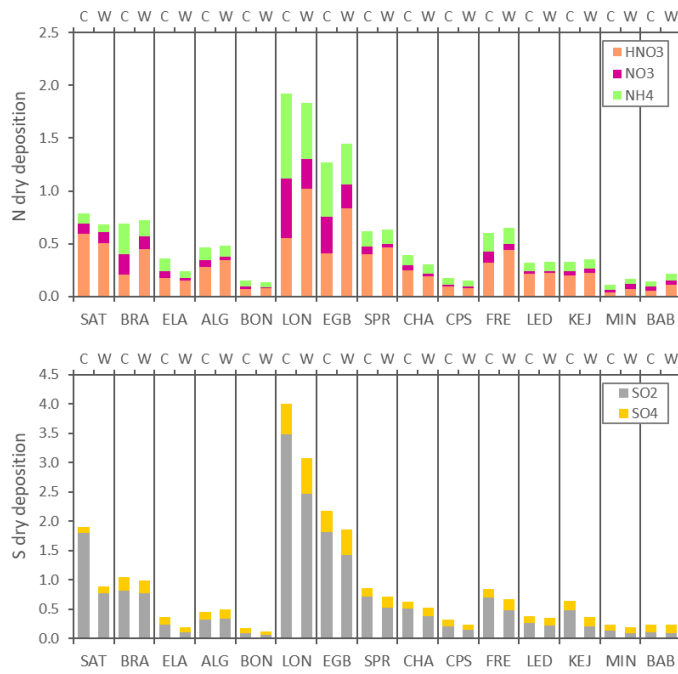


**Figure 3: Mean dry deposition fluxes of N and S species (kg N or S ha⁻¹ yr⁻¹) during the cold (Nov-Apr) and warm (May-Oct) seasons during 2000-2018. C: cold season; W: warm season.**

380

### 3.2.3 Long-term annual trends

Long-term trends in annual dry deposition of total N and S at 15 CAPMoN sites estimated using Theil-Sen slopes are shown in Fig. 4 and 5, respectively. The rate of decrease in annual dry N deposition ranged from -0.007 (BON) to -0.11 (LON) kg N ha⁻¹ yr⁻¹. This is equivalent to percentage decreases of -2.6% to -5.0% per year (Table S4). The largest rate of decline in 385 N dry deposition was at the two sites in southeastern Canada, LON and EGB (Fig. 4). Greater interannual variability in N dry fluxes at these two sites was due to the larger variability in their ambient concentrations. Ambient N concentrations at these two locations have been the highest among CAPMoN sites since measurements began in 1983 (Cheng and Zhang, 2017) because of the strong influence of local urban and transboundary pollution. In the last two decades, ambient N concentrations have decreased significantly as a result of air pollution control measures aimed at reducing NO<sub>x</sub> emissions in 390 Canada and the U.S (section 3.1). This improvement in air quality was largely responsible for the decrease in dry deposition of N and S. The reductions in dry deposition fluxes were not attributed to changes in annual V<sub>d</sub> of N and S species based on Theil-Sen's analysis (Section S1.3; Fig. S2). Moderate rates of decline in dry deposition of N were observed in the greater southeastern region (SPR, FRE, CHA, ALG), west coast (SAT) and in the Atlantic region (LED, KEJ). Weak declining trends were estimated at remote sites (ELA, BON, CPS, BAB), where the ambient N concentrations have always been the 395 lowest in Canada. Thus, the interannual variability at remote sites were also much smaller compared with southeastern



Canadian sites. Although the absolute rates of decrease were small, the percentage reductions in dry N deposition across Canada were substantial (Table 2). No trends were found at BRA and MIN.

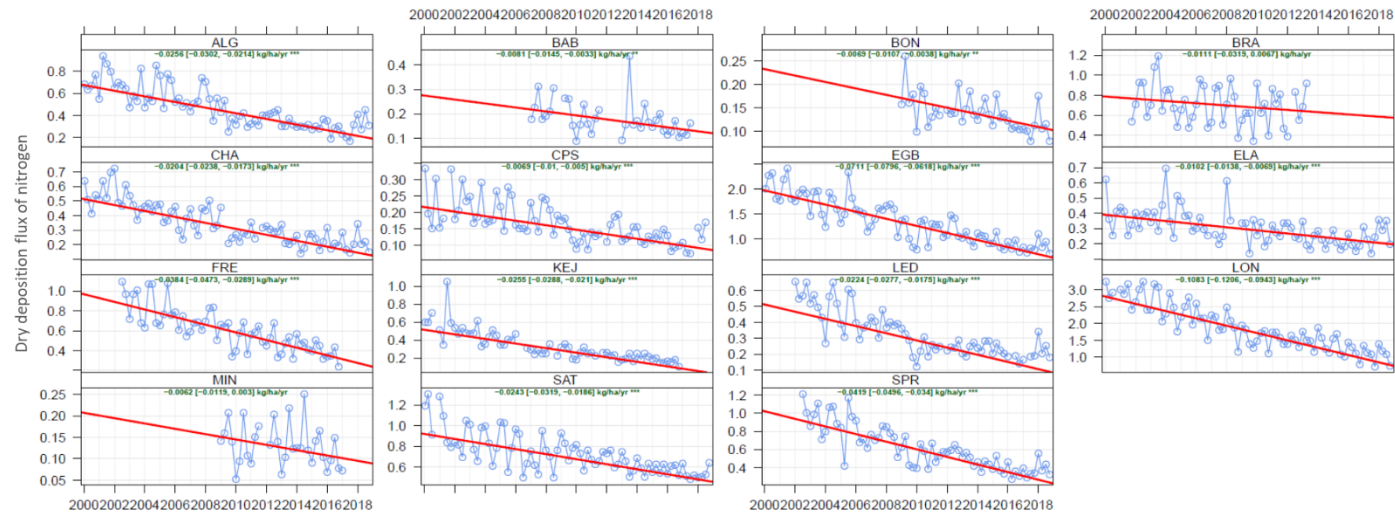


Figure 4: Annual trends in dry deposition fluxes of nitrogen at CAPMoN sites ( $\text{kg N ha}^{-1} \text{yr}^{-1}$ ). Theil-Sen slope and 95% confidence interval (green text); trendline de-seasonalized using LOESS (red line); observed seasonal mean dry deposition fluxes (blue time-series). Note: excludes  $\text{NH}_3$  and other  $\text{NO}_y$  dry deposition. Statistically significant trends shown with \*\*\* ( $p < 0.001$ ) or \*\* ( $p < 0.01$ ). 

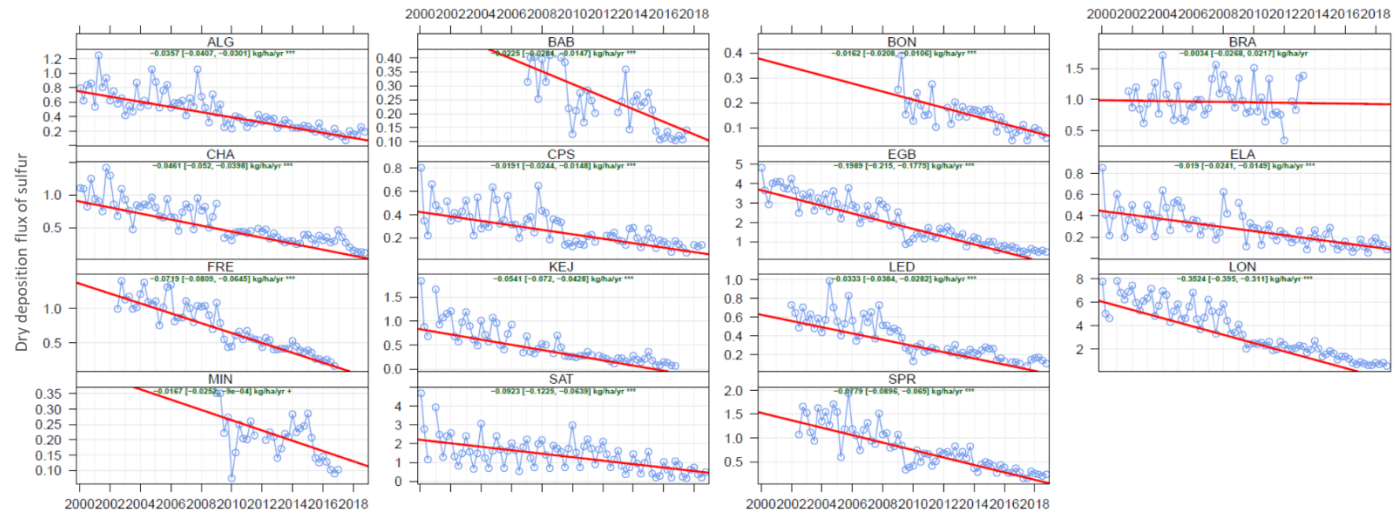


Figure 5: Annual trends in dry deposition fluxes of sulfur at CAPMoN sites ( $\text{kg S ha}^{-1} \text{yr}^{-1}$ ). Theil-Sen slope and 95% confidence interval (green text); trendline de-seasonalized using LOESS (red line); observed seasonal mean dry deposition fluxes (blue time-series). Statistically significant trends shown with \*\*\* ( $p < 0.001$ ) or + ( $p < 0.1$ ). 



At LON, EGB and FRE, the decreasing trends in dry N deposition from 2000-2018 were driven by the decrease in  $\text{HNO}_3$  and  $\text{pNH}_4^+$  dry deposition. The rates of decline in dry N deposition ( $\text{kg N ha}^{-1} \text{yr}^{-1}$ ) from  $\text{HNO}_3$  and  $\text{pNH}_4^+$ , respectively, were -0.040 and -0.043 at LON, -0.027 and -0.027 at EGB, and -0.025 and -0.011 at FRE (Fig. S6). In other parts of Canada, the decrease in dry N deposition was largely due to those of  $\text{HNO}_3$ , while  $\text{pNH}_4^+$  and  $\text{pNO}_3^-$  showed a very weak trend. As reported by Feng et al. (2020), there was also a lack of trend in the annual mean concentrations of  $\text{pNO}_3^-$  in eastern Canada and the eastern U.S. except for the Midwest.

415

The annual rate of decrease in dry deposition of S was greater than that of N at all sites, which was consistent with the trends in their ambient air concentrations. The rates of decrease varied from -0.016 (BON) to -0.35 (LON)  $\text{kg S ha}^{-1} \text{yr}^{-1}$  (4.2% to -7.1% per year; Fig. S6 and Table S4). Similar to dry N deposition, the steepest declines in dry S deposition were found at LON and EGB (Fig. 5). Rates of decrease in dry S deposition were also substantial at the west coast site (SAT) and the greater southeastern region (SPR, FRE). Moderate decreasing trends in dry S deposition were found at other southeastern Canadian sites (ALG, CHA) and in the Atlantic region (LED, KEJ). Remote sites including ELA, BON, CPS and BAB exhibited weak temporal trends in dry S deposition. No trends in dry S deposition were found at BRA and MIN.

425 Although the overall trends are shown in Fig. 4 and 5, there were differences in the rates of decline in N and S annual dry deposition for the periods before and after 2010. Annual dry N deposition decreased more rapidly during 2000-2009 compared to 2010-2018 (Table 4). Based on eleven sites with sufficient pre- and post- 2010 data, the rate of change in annual dry N deposition ranged from -0.009 to -0.16  $\text{kg N ha}^{-1} \text{yr}^{-1}$  pre-2010 and -0.009 to -0.08  $\text{kg N ha}^{-1} \text{yr}^{-1}$  post-2010. The magnitude of the trend at LON after 2010 was half of that before 2010. Furthermore at 3 of the 11 sites (ELA, CPS, LED), the trends in annual dry N deposition were not statistically significant for the period after 2010. The current trend in 430 annual dry N deposition appears to be weakening across Canada, which is similar to the  $\text{NO}_x$  emissions trends in Canada (section 3.1). There was also a shift in the N compounds driving the declines in annual dry N deposition before and after 2010. At LON and EGB, the dry N deposition trends were equally dominated by those of  $\text{HNO}_3$  and  $\text{pNH}_4^+$  during 2000-2009. After 2010, the trends in  $\text{HNO}_3$  dry deposition plateaued and those of  $\text{pNH}_4^+$  drove the weaker dry N deposition trends in this period (Table 4). This result was likely attributed to the flattening in  $\text{NO}_x$  emissions. Meanwhile, as  $\text{SO}_2$  ambient 435 concentrations continued to decline after 2010, the secondary formation of  $\text{pNH}_4^+$  was also reduced. Ambient  $\text{NH}_3$  monitoring would be required to [confirm the future](#) trends in N dry deposition.

440 For annual dry S deposition, the rate of decrease was much slower during 2010-2018 compared to the previous decade (Table 4). For example, the magnitude of the trends at LON and EGB were 50-60% of that in the previous decade. This was due to the weaker trend in ambient  $\text{SO}_2$  concentrations after 2010, which can be traced back to a similar weak trend in  $\text{SO}_x$  emissions in Ontario and Quebec. Interestingly, the rate of decline in annual dry S deposition accelerated after 2010 at SAT and ELA (Table 4). Prior to 2010, the trends were not statistically significant at either site.



445 **Table 4: Rate of change in annual dry deposition fluxes of N and S species (kg N or S ha<sup>-1</sup> yr<sup>-1</sup>)** based on Theil-Sen slopes (statistically significant at p<0.05). Pre 2010: 2000-2009 period; post 2010: 2010-2018 period; NA: not available due to incomplete data; ns: trend is not statistically significant. Note:  $\Sigma$ Nitrogen excludes dry deposition of NH<sub>3</sub> and some oxidized nitrogen species.

Site	HNO <sub>3</sub>		pNH <sub>4</sub> <sup>+</sup>		pNO <sub>3</sub> <sup>-</sup>		SO <sub>2</sub>		pSO <sub>4</sub> <sup>2-</sup>		$\Sigma$ N		$\Sigma$ S	
	pre 2010	post 2010	pre 2010	post 2010	pre 2010	post 2010	pre 2010	post 2010	pre 2010	post 2010	pre 2010	post 2010	pre 2010	post 2010
SAT	-0.024	-0.014	ns	-0.005	-0.004	ns	ns	-0.167	-0.004	-0.007	-0.032	-0.021	ns	-0.172
BRA	ns	NA	ns	NA	ns	NA	ns	NA	ns	NA	ns	NA	ns	NA
ELA	-0.009	ns	ns	ns	ns	ns	ns	-0.013	-0.005	-0.004	-0.011	ns	ns	-0.018
ALG	-0.025	-0.008	-0.005	-0.003	ns	ns	-0.025	-0.022	-0.008	-0.006	-0.032	-0.009	-0.033	-0.028
BON	NA	-0.003	NA	-0.003	NA	ns	NA	-0.010	NA	-0.006	NA	-0.006	NA	-0.016
LON	-0.059	ns	-0.055	-0.037	-0.040	ns	-0.361	-0.207	-0.042	-0.032	-0.155	-0.078	-0.404	-0.239
EGB	-0.035	ns	-0.031	-0.021	-0.028	ns	-0.220	-0.117	-0.030	-0.023	-0.095	-0.062	-0.253	-0.133
SPR	-0.059	-0.020	-0.013	-0.007	ns	ns	-0.097	-0.052	-0.018	-0.011	-0.071	-0.031	-0.116	-0.061
CHA	-0.021	-0.006	-0.006	-0.004	ns	ns	-0.043	-0.023	-0.009	-0.006	-0.029	-0.012	-0.056	-0.030
CPS	-0.006	ns	ns	ns	ns	ns	-0.018	ns	-0.006	ns	-0.009	ns	-0.024	-0.008
FRE	-0.041	ns	-0.009	-0.011	ns	ns	-0.057	-0.050	ns	-0.012	-0.047	-0.032	-0.069	-0.062
LED	-0.033	ns	-0.006	ns	ns	ns	-0.031	-0.014	-0.010	-0.004	-0.042	ns	-0.037	-0.019
KEJ	-0.029	-0.009	-0.006	-0.006	ns	ns	-0.066	-0.018	-0.017	-0.010	-0.039	-0.018	-0.081	-0.028
MIN	NA	ns	NA	ns	NA	ns	NA	ns	NA	ns	NA	ns	NA	ns
BAB	NA	ns	NA	ns	NA	ns	NA	-0.008	NA	-0.008	NA	ns	NA	-0.016

### 3.3 Total deposition fluxes

#### 3.3.1 Geographical distribution

450 Total deposition fluxes were obtained by summing the dry deposition flux estimates and wet deposition measurements. Total deposition fluxes of N and S during 2000-2018 ranged from 1.7 to 9.5 kg N ha<sup>-1</sup> yr<sup>-1</sup> and from 1.3 to 8.5 kg S ha<sup>-1</sup> yr<sup>-1</sup> across Canada. The fluxes in Canada were lower than those in the continental U.S. over a similar timeframe (2002-2017), namely 3.3-11 kg N ha<sup>-1</sup> yr<sup>-1</sup> and 1-11 kg S ha<sup>-1</sup> yr<sup>-1</sup> which includes NH<sub>3</sub> and other oxidized nitrogen (Benish et al., 2022). Total N and non-sea salt S deposition were highest in the southeastern region and were comparable among west coast, prairie, remote continental and Atlantic region sites (Table 5). As illustrated in Fig. 6, the percentage of oxidized and reduced N were similar in the southeastern region; however, oxidized N does not include NO<sub>2</sub> dry deposition and reduced N does not include NH<sub>3</sub> dry deposition. Oxidized N was greater than reduced N deposition at the west coast site and in the 455 Atlantic region, while reduced N exceeded oxidized N at the prairie and remote continental sites (Fig. 6).

460 The inclusion of NO<sub>2</sub>, NH<sub>3</sub>, PAN and unknown NO<sub>y</sub> dry deposition increased the total N deposition during the 2002-2005 period from 4.2-9.5 kg N ha<sup>-1</sup> yr<sup>-1</sup> (routinely-monitored N) to 4.6-11.6 kg N ha<sup>-1</sup> yr<sup>-1</sup>, depending on the site (Zhang et al., 2009). The increase in total N deposition due to the inclusion of NO<sub>2</sub>, NH<sub>3</sub>, PAN and unknown NO<sub>y</sub> dry deposition was



greater at CAPMoN sites near agricultural areas ( $\sim 1.7 \text{ kg N ha}^{-1} \text{ yr}^{-1}$  increase) compared with other sites ( $\sim 0.4 \text{ kg N ha}^{-1} \text{ yr}^{-1}$  increase) (Zhang et al., 2009). At the EGB site, which is surrounded by agricultural areas,  $\text{NH}_3$  dry deposition was a significant contributor to total N deposition. Dry deposition of the non-routinely monitored species increased the total N deposition at EGB from  $5.2 \text{ kg N ha}^{-1}$  (routinely-monitored N) to  $7.75 \text{ kg N ha}^{-1}$  in 2010 (Table 3). Note that the N dry deposition of the non-routinely monitored species at EGB in 2010 was only  $\sim 0.3 \text{ kg N ha}^{-1} \text{ yr}^{-1}$  higher than that in 2002. This was because the increase in  $\text{NH}_3$  dry deposition from 2002 to 2010 was largely offset by the decrease in  $\text{NO}_2$  dry deposition. The importance of agricultural  $\text{NH}_3$  to local and downwind total N deposition is evident (Walker et al., 2019; Hu et al., 2021; Pan et al., 2021); however, quantifying its role remains elusive in natural lands in Canada because of limited measurements.

In the early 2000s, total N deposition fluxes were comparable by mass to those of total S (Table 5). During the latter period in 2014-2018, total N deposition exceeded that of total S in most regions. This is due to the large declines in ambient S from the early 2000s to the recent period. Significant declines in total N and S deposition were observed between the two periods with percentage decreases of 19-37% and 54-71%, respectively (Table 2). Oxidized N (i.e. dry  $\text{HNO}_3$  + dry  $\text{pNO}_3^-$  + wet  $\text{NO}_3^-$ ) deposition was greater than that of reduced N (i.e. dry  $\text{pNH}_4^+$  + wet  $\text{NH}_4^+$ ) during 2000-2004 in all regions (Table 5). During 2014-2018, reduced N deposition surpassed oxidized N deposition in the southeastern region; however, oxidized N deposition continued to be greater than reduced N deposition in the west coast, prairie, and Atlantic regions.

480

**Table 5: Regional breakdown of mean total (dry+wet) N and S deposition fluxes ( $\text{kg N or S ha}^{-1} \text{ yr}^{-1}$ ) across Canada**

Region (site ID)	Period	Total S <sup>a</sup>	Total N	$\text{NO}_3^-$ (oxidized N <sup>b</sup> )	$\text{NH}_4^+$ (reduced N <sup>c</sup> )
Southeastern (LON, EGB)	2000-2018	5.7-8.5	7.1-9.5	3.6-4.7	3.5-4.8
	2000-2004	8.4-12.9	8.3-11.6	4.7-6.4	3.6-5.2
	2014-2018	2.5-3.8	6.3-7.9	2.6-3.3	3.7-4.6
Greater southeastern (SPR, ALG, CHA, FRE)	2000-2018	4.5-5.1	5.1-7.7	2.7-3.7	2.4-4.0
	2000-2004	5.4-7.0	6.3-9.6	3.7-5.0	2.6-4.6
	2014-2018	1.8-2.8	4.0-6.4	1.9-2.9	2.1-3.7
West coast & prairie (SAT, BRA)	2000-2018	2.1-2.4	2.6-3.2	1.4-1.8	0.7-1.9
	2000-2004	1.8-3.3	2.9-3.4	1.3-2.1	0.8-1.5
	2014-2018	1.3	2.2	1.5	0.7
Atlantic (KEJ, MIN, BAB)	2000-2018	1.5-3.0	1.7-3.3	1.0-2.0	0.6-1.2
	2000-2004	3.3	4.0	2.7	1.3
	2014-2018	1.1-1.5	1.4-2.6	0.9-1.5	0.6-1.1



Remote continental (ELA, BON, CPS, LED)	2000-2018	1.3-2.9	2.8-4.0	1.2-2.2	1.5-2.4
	2000-2004	2.2-4.0	4.0-5.1	2.0-3.1	1.8-2.5
	2014-2018	1.0-1.8	2.6-3.7	1.2-1.8	1.3-2.4

<sup>a</sup> Total S includes dry SO<sub>2</sub>, dry pSO<sub>4</sub><sup>2-</sup>, and wet SO<sub>4</sub><sup>2-</sup>

<sup>b</sup> Oxidized N includes dry HNO<sub>3</sub>, dry pNO<sub>3</sub><sup>-</sup>, and wet NO<sub>3</sub><sup>-</sup>

<sup>c</sup> Reduced N includes dry pH<sub>4</sub><sup>+</sup> (no NH<sub>3</sub>) and wet NH<sub>4</sub><sup>+</sup>

485

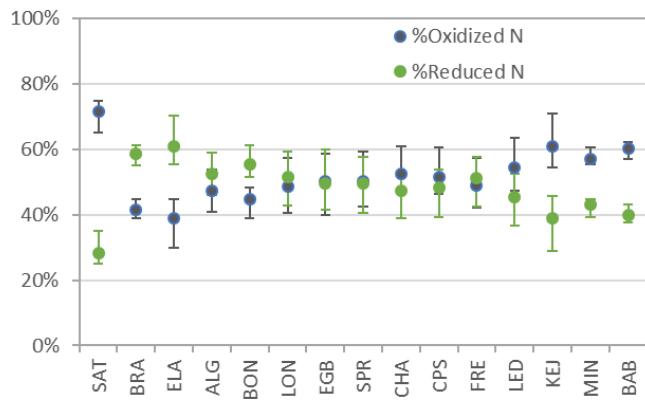


**Figure 6: Percentage of oxidized and reduced N species in annual total deposition of N during 2000-2018. Mean (circle); range or annual variability (error bars).**

490 **3.3.2 Relative contributions of dry and wet deposition**

Total N deposition was dominated by wet deposition of NO<sub>3</sub><sup>-</sup> and NH<sub>4</sub><sup>+</sup>, while total S deposition was dominated by wet deposition of SO<sub>4</sub><sup>2-</sup> and dry deposition of SO<sub>2</sub>. Annual wet deposition of total N and S averaged over all years were greater than those of dry deposition. Wet N deposition ranged from 71 to 95% depending on the location (Fig. 7), while wet S deposition varied from 45 to 89%. At the west coast, prairie, and southeastern sites, the relative contribution from dry deposition was slightly higher compared with other sites (Fig. 7). This is due to the lower precipitation amounts in the west coast and prairie sites and the higher atmospheric N and S concentrations at the two southeastern sites. At EGB, the relative wet and dry N deposition of routine species were 79% and 21%, respectively, in 2010. With the inclusion of dry deposition of NO<sub>2</sub>, NH<sub>3</sub> and unknown NO<sub>y</sub>, the relative N dry deposition increased to 47%. The relative total N deposition in 2010 was dominated by NH<sub>4</sub><sup>+</sup> wet deposition, NH<sub>3</sub> dry deposition and NO<sub>3</sub><sup>-</sup> wet deposition (Table 3), whereas in 2002, NH<sub>4</sub><sup>+</sup> and NO<sub>3</sub><sup>-</sup> wet deposition and NO<sub>y</sub> dry deposition comprised the bulk of total N deposition (Zhang et al., 2009). A comparison between 495 2002 and 2010 shows a clear shift from the predominance of oxidized N to reduced N in total deposition at EGB if NH<sub>3</sub> dry deposition is accounted for.

500



Ratios of wet to dry deposition fluxes varied between sites. On average, wet deposition exceeded dry deposition by a factor of 10 for total N and a factor of 5 for total S. There were also large differences between wet and dry deposition of oxidized and reduced N. Mean wet/dry flux ratios for oxidized and reduced N were ~7 (range: 1.7 to 14.7, depending on location) and ~18 (range: 6.2 to 32.9), respectively. The large disparity between wet and dry deposition of reduced N was likely because of the lack of data on dry  $\text{NH}_3$  deposition and the minor contribution to dry deposition from  $\text{pNH}_4^+$ . For example, the wet/dry flux ratio for reduced N at EGB in 2010 was 7.2 without considering  $\text{NH}_3$  dry deposition, whereas the ratio was only 1.0 after including  $\text{NH}_3$  dry deposition. Thus, the actual ratio should be between 1.0 and 7.2 if bi-directional exchange is considered for  $\text{NH}_3$ .

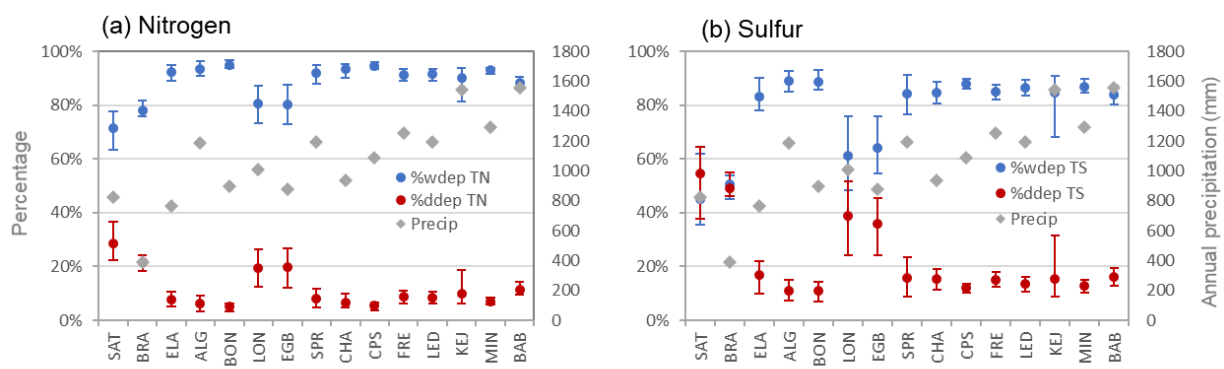


**Figure 7: Percentage of wet and dry annual deposition of (a) nitrogen and (b) sulfur during 2000-2018. Mean percentage (circles); range or annual variability in the percentage (error bars); mean annual precipitation amount (diamonds).**

515

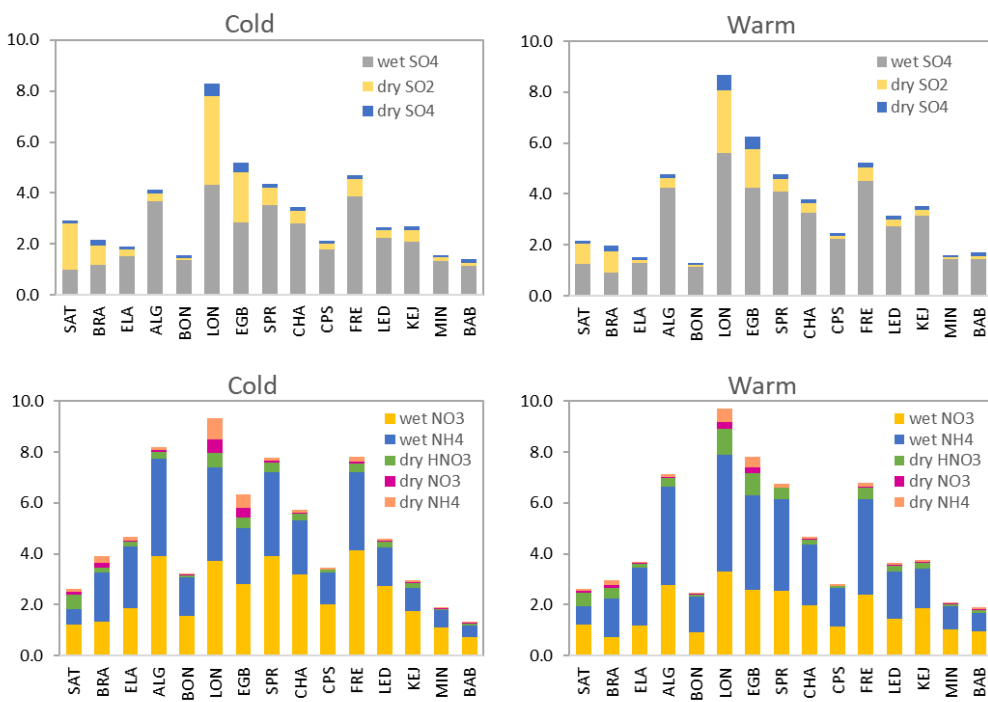
### 3.3.3 Seasonal patterns

Mean total deposition of N, the mean cold and warm season fluxes were  $1.4$  to  $9.3 \text{ kg N ha}^{-1} \text{ yr}^{-1}$  and  $1.9$  to  $9.7 \text{ kg N ha}^{-1} \text{ yr}^{-1}$ . Larger differences in the fluxes between seasons were observed for N deposition. Notably, mean total N deposition in the cold season was greater than in the warm season by  $\sim 1 \text{ kg N ha}^{-1} \text{ yr}^{-1}$  at BRA, ELA, ALG, SPR, CHA, FRE and LED (Fig. 520 S7). At EGB, the warm season flux exceeded the cold season flux by  $1.5 \text{ kg N ha}^{-1} \text{ yr}^{-1}$ . Total N deposition was dominated by wet  $\text{NO}_3^-$  in the cold season and by wet  $\text{NH}_4^+$  in the warm season (Fig. 8). Wet  $\text{NO}_3^-$  deposition was greater in the cold season than in the warm season and vice versa for wet  $\text{NH}_4^+$  deposition. The proportion from dry N deposition (i.e.  $\text{HNO}_3 + \text{pNO}_3^- + \text{pNH}_4^+$ ) was similar between the cold and warm season at most sites.

525 Mean total deposition of S ranged from  $1.4$  to  $8.3 \text{ kg S ha}^{-1} \text{ yr}^{-1}$  during the cold season and  $1.3$  to  $8.7 \text{ kg S ha}^{-1} \text{ yr}^{-1}$  during the warm season. The differences in the total S flux between seasons were larger at a few sites. The cold season flux was  $0.75 \text{ kg S ha}^{-1} \text{ yr}^{-1}$  greater than the warm season flux at SAT, whereas the warm season flux was  $1.1 \text{ kg S ha}^{-1} \text{ yr}^{-1}$  greater than the



530 cold season flux at EGB (Fig. S8). Wet  $\text{SO}_4^{2-}$  deposition dominated the total deposition of S at most sites in either season, except for the west coast and prairie sites and two southeastern sites. At these sites, dry S and wet  $\text{SO}_4^{2-}$  deposition were nearly equivalent during the cold season (Fig. 8). Wet  $\text{SO}_4^{2-}$  deposition was greater while dry S deposition was smaller in the warm season than in the cold season.



535 **Figure 8: Mean total (dry+wet) deposition fluxes of N and S species in  $\text{kg N or S ha}^{-1} \text{yr}^{-1}$  during the cold (Nov-Apr) and warm (May-Oct) seasons during 2000-2018.**

### 3.3.4 Long-term annual trends

Long-term trends in annual total (dry+wet) deposition of N, non-sea salt S and individual components are shown in Fig. 9 and 10, respectively. Based on Mann-Kendall analyses, statistically significant decreasing trends in total N deposition were found at 11 sites with slopes ranging from -0.03 (SAT) to -0.25 (LON)  $\text{kg N ha}^{-1} \text{yr}^{-1}$  (Table 6). This is equivalent to decreasing trends of -1.1% to -3.3% per year for total N deposition (Table S4). Over the continental U.S., total N deposition 540 also decreased at a similar rate of -0.06 to -0.3  $\text{kg N ha}^{-1} \text{yr}^{-1}$  during the same period owing to  $\text{NO}_x$  emissions reductions (Benish et al., 2022). Annual trends were not significant at BON, MIN and BAB ( $p>0.05$ ). Decreasing trends in total deposition of S were found at 14 sites with magnitudes ranging from -0.08 (ELA) to -0.66 (LON)  $\text{kg S ha}^{-1} \text{yr}^{-1}$  (-3.5% to -6.6% per year). Annual trends in total N and S deposition were not available at BRA due to data gaps. Total deposition fluxes of N and S declined more rapidly in southeastern Canada than in the Atlantic region and remote sites, which reflect 545 the substantial  $\text{NO}_x$  and  $\text{SO}_2$  emissions reductions in eastern Canada and the eastern U.S. (Fig. S5a). Total N and S



deposition at the west coast site decreased at a slower rate compared with southeastern Canada. This result is consistent with the slower decline in emissions reductions in western Canada (Fig. S5b). Oxidized N compounds drove the decreasing trends in total deposition of N at the majority of the sites (Table 6). Trends in reduced N were not statistically significant at most sites except for the slight decreasing trends at ALG, CHA and CPS.

550

The lack of trends in total deposition of reduced N (excluding dry deposition of  $\text{NH}_3$ ) can be explained as follows. First, total deposition of reduced N was dominated by the wet deposition of  $\text{NH}_4^+$ , which exhibited a lack of trend in the eastern U.S. and eastern Canada (Feng et al., 2021). Second, although ambient concentrations of  $\text{pNH}_4^+$  decreased as a result of declines in  $\text{pSO}_4^{2-}$  and  $\text{pNO}_3^-$ , dry deposition of  $\text{pNH}_4^+$  was relatively less important as  $\text{pNH}_4^+$  was predominately in  $\text{PM}_{2.5}$  which has a smaller  $V_d$  compared with coarse or ultrafine particulates ( $d < 0.1 \mu\text{m}$ ) (Zhang and He, 2014). However, with less  $\text{pNH}_4^+$  formed in the air due to  $\text{SO}_2$  and  $\text{NO}_x$  emissions reductions, ambient  $\text{NH}_3$  in the air increased over the U.S. and Canada (Butler et al., 2016; Yao and Zhang, 2016; Feng et al., 2021). This is possible given that the  $V_d$  of  $\text{NH}_3$  is 5 to 10 times higher than the  $V_d$  of  $\text{pNH}_4^+$ ; however, additional long-term measurements of ambient  $\text{NH}_3$  would be required in order to verify this (e.g., via ongoing remote sensing and passive measurements).

560

Similar to the trends in dry deposition, differences in the annual total deposition trends were observed between the 2000-2009 period and 2010-2018 period. While the decreasing trends in total deposition of N were statistically significant at eight sites in the period before 2010, there were only two sites with significant declining trends after 2010 (Table 6). Relatively flat trends in ambient  $\text{TNO}_3$  ( $\text{pNO}_3^- + \text{HNO}_3$ ) were also reported for the Northeast, the Mid-Atlantic and the Southeast of the U.S. after 2010 (Feng et al., 2020). Prior to 2010, long-term trends in total deposition of N were mainly driven by oxidized N species. Trends in reduced N deposition were not statistically significant in either period. Decreasing trends in total deposition of S were statistically significant in the periods before and after 2010. The magnitude of the trends were smaller during 2010-2018 compared with 2000-2009 at ALG, EGB, SPR and LED, whereas the trends during 2010-2018 were equal to or larger than those during 2000-2009 at SAT, LON, CHA, and FRE (Table 6). During the last decade, total deposition of S has continued to decrease owing to reductions in  $\text{SO}_2$  emissions. In contrast, total deposition of N and  $\text{NO}_x$  emissions have leveled off in the last decade in Canada, similar to the continental U.S. (Benish et al., 2022).

570 **Table 6: Rate of change in annual total (dry+wet) deposition fluxes of N and S ( $\text{kg N or S ha}^{-1} \text{yr}^{-1}$ ) based on Theil-Sen slopes (statistically significant at  $p < 0.05$ ). Pre 2010: 2000-2009 period; post 2010: 2010-2018 period; NA: not available due to incomplete data; ns: trend is not statistically significant. Note: Total N and reduced N exclude dry deposition of  $\text{NH}_3$  and some oxidized nitrogen species.**

Site	2000-2018				Total S		Total N		Total oxidized N		Total reduced N	
	Total S	Total N	Total oxidized N	Total reduced N	pre 2010	post 2010	pre 2010	post 2010	pre 2010	post 2010	pre 2010	post 2010



SAT	-0.14	-0.03	-0.03	ns	-0.10	-0.22	ns	ns	ns	ns	ns	ns
BRA	NA											
ELA	-0.08	-0.06	-0.05	ns	ns	-0.06	ns	ns	-0.08	ns	ns	ns
ALG	-0.29	-0.24	-0.19	-0.07	-0.34	-0.26	-0.38	ns	-0.27	ns	ns	ns
BON	-0.10	ns	ns	ns	NA	-0.10	NA	ns	NA	ns	NA	ns
LON	-0.66	-0.25	-0.22	ns	-0.59	-0.57	-0.41	ns	-0.31	-0.14	ns	ns
EGB	-0.40	-0.16	-0.15	ns	-0.38	-0.28	-0.21	ns	-0.20	ns	ns	ns
SPR	-0.37	-0.20	-0.17	ns	-0.47	-0.34	-0.39	ns	-0.32	-0.11	ns	ns
CHA	-0.25	-0.15	-0.12	-0.03	-0.23	-0.26	ns	-0.22	-0.16	-0.11	ns	-0.09
CPS	-0.17	-0.14	-0.09	-0.04	-0.19	-0.16	-0.23	-0.14	-0.13	ns	ns	ns
FRE	-0.38	-0.16	-0.15	ns	ns	-0.37	-0.33	ns	-0.26	ns	ns	ns
LED	-0.18	-0.13	-0.11	ns	-0.21	-0.15	-0.31	ns	-0.23	ns	-0.08	ns
KEJ	-0.21	-0.11	-0.09	ns	-0.23	-0.19	-0.20	ns	-0.18	ns	ns	ns
MIN	-0.12	ns	ns	ns	NA	-0.14	NA	ns	NA	ns	NA	ns
BAB	-0.16	ns	ns	ns	NA	-0.15	NA	ns	NA	ns	NA	ns

A comparison of dry and wet deposition trends indicates that wet deposition of oxidized N and  $\text{SO}_4^{2-}$  decreased more rapidly  
580 than dry deposition from 2000 to 2018, although differences between wet and dry deposition trends varied across locations. Trends in the wet deposition of oxidized N ( $\text{NO}_3^-$ ) were much greater than those of dry deposition ( $\text{HNO}_3 + \text{pNO}_3^-$ ). Depending on the site, the annual rate of decrease in wet deposition of oxidized N was greater than dry deposition of oxidized N by a factor of 2.5 (LON and EGB) to 17 (CPS). The annual rate of decrease in wet deposition of  $\text{SO}_4^{2-}$  exceeded that of dry deposition ( $\text{SO}_2 + \text{pSO}_4^{2-}$ ) by a factor of 1.1 (EGB) to 7.9 (CPS) (Table S5). In contrast, decreasing trends in dry  
585 deposition of S were greater than those of wet deposition at SAT and LON. The inter-site variability between wet versus dry deposition trends is likely due to the distance from emission sources. The  $\text{SO}_2$  and  $\text{NO}_x$  concentrations and by extension dry deposition are quite low at remote sites. Thus, decreasing emissions from distant sources have minor impact on the ambient concentrations and dry deposition. Trends in the emissions at remote sites are mostly reflected in wet deposition given the high precipitation amounts at these sites (Fig. 9 and 10). While there were slight decreasing trends in dry deposition of  
590  $\text{pNH}_4^+$  at all CAPMoN sites, trends in annual wet deposition of reduced N ( $\text{NH}_4^+$ ) were not significant at most of the Canadian sites (Table S5). The rate of decline in wet deposition fluxes were greater than those of dry fluxes for N and S based on the absolute fluxes. However, the percentage decrease in dry deposition was greater than those in wet deposition (Table 2) owing to the smaller magnitude of dry fluxes compared to wet fluxes. The percentage decreases in dry deposition of S and oxidized N between 1990 and 2010 were also greater than that of wet deposition in the U.S. (Sickles and Shadwick,  
595 2015; Zhang et al., 2018). Changes in the meteorological conditions, especially the precipitation amount, may have played a role in the different trends and their relative dry and wet contributions to total deposition, but this is outside the scope of this paper and could be the subject of future analysis.



The proportion of total deposition of N and S from wet deposition increased modestly during the 2000-2018 period (Table 600 S5). The increasing trends were statistically significant at 11 sites with the percentage of wet N in total deposition varying from 0.1%/yr (ELA) to 0.5-0.6%/yr (SAT, LON, EGB). For the percentage of wet S in total deposition, the trends were statistically significant at 10 sites and the magnitudes ranged from 0.2%/yr (ELA) to 1.3%/yr (LON). Long-term trends in the percentages of oxidized and reduced N in total deposition were also analyzed. Due to significant decreases in oxidized N 605 deposition and lack of trend in reduced N deposition during 2000-2018, the proportion of reduced N in total deposition have generally risen over the same period. Increasing trends in the percentage of reduced N in total deposition were estimated at 11 sites with magnitudes ranging from 0.3%/yr to 1.3%/yr. The largest rates of increase (>1% reduced N/yr) were found at EGB, FRE, LON, SPR and LED (Table S5). The rise in the percentage of reduced N is a conservative estimate since NH<sub>3</sub> dry deposition was not included.



610  
**Figure 9: Long-term annual trends in total (dry+wet) deposition of nitrogen.** Total deposition (kg N ha<sup>-1</sup> yr<sup>-1</sup>, primary y-axis); precipitation (mm yr<sup>-1</sup>, secondary y-axis); \* indicates dry or wet deposition data were not available because data completeness criteria were not met.

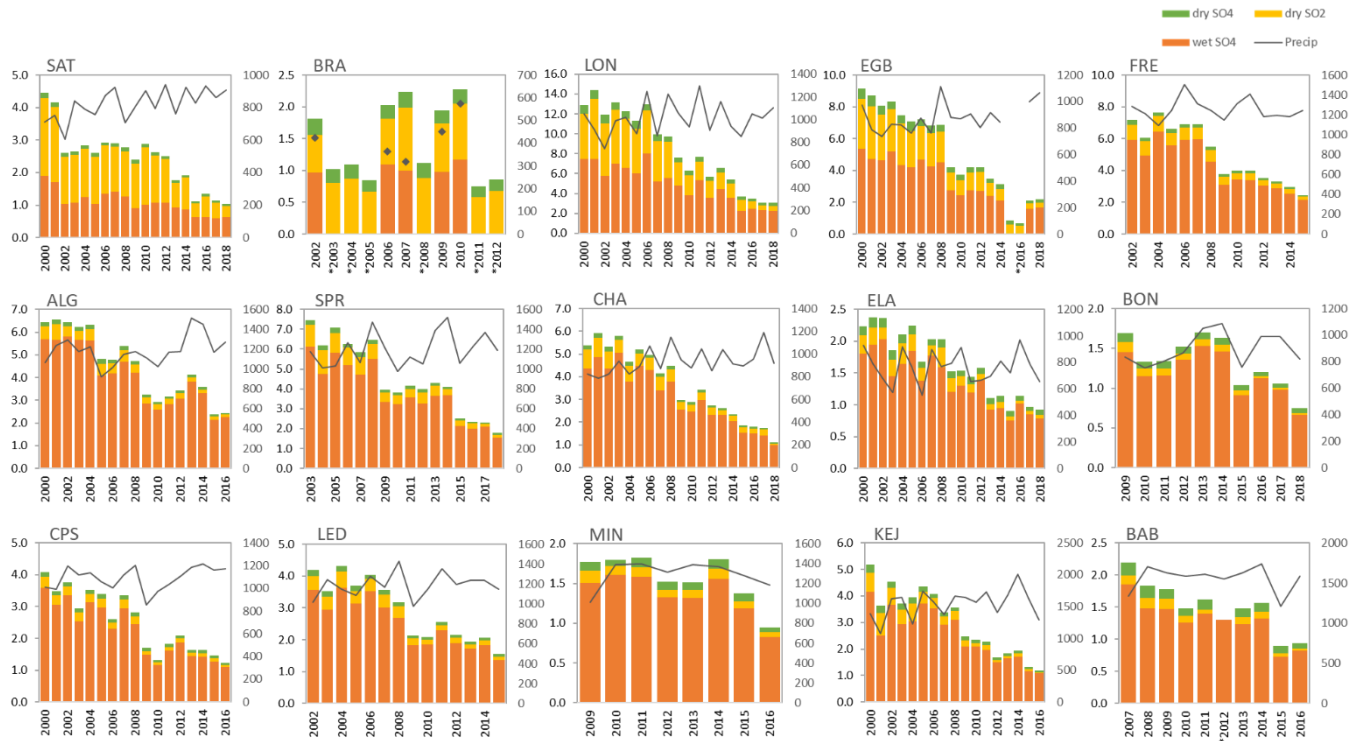


Figure 10: Long-term annual trends in total (dry+wet) deposition of sulfur. Total deposition ( $\text{kg S ha}^{-1} \text{yr}^{-1}$ , primary y-axis); precipitation ( $\text{mm yr}^{-1}$ , secondary y-axis); \* indicates dry or wet deposition data were not available because data completeness criteria were not met.

615

## 620 3.4 N and S deposition response to long-term changes in emissions

The efficacy of emissions reductions were evaluated by examining the ratio of the percentage change in deposition of N and S to the percentage change in precursor emissions based on the Theil-Sen's slopes (i.e. response). Analysis of emissions changes were based on emissions from the large geographical regions that are known to influence the CAPMoN sites according to previous back trajectory analyses. This approach increased the likelihood of detecting relationships between 625 ambient measurements and emissions by reducing the local meteorological effects on the ambient measurements (Brook et al., 1994). Wet  $\text{NO}_3^-$  deposition has declined drastically in the U.S. northeast owing to large reductions in  $\text{NO}_x$  emissions (Du et al., 2014; Li et al., 2016), and the response in total oxidized N deposition to changes in  $\text{NO}_x$  emissions between 2000 and 2017 was nearly 1 to 1 based on model simulations (Nopmongcol et al., 2019; Tan et al., 2020). A similar analysis spanning the early 1990s to mid-2000s indicated that the response in total oxidized N deposition to  $\text{NO}_x$  emissions decrease 630 in the eastern U.S. was closer to 65-78% (Sickles and Shadwick, 2015). In the southeastern U.K., the response in wet  $\text{NO}_3^-$  concentrations to domestic  $\text{NO}_x$  emissions reductions was 0.8 to 1 based on a 20% change in wet  $\text{NO}_3^-$  and 25% change in  $\text{NO}_x$  emissions (Fowler et al., 2005). In this study, we estimated that the response in total oxidized N deposition to  $\text{NO}_x$



emissions reductions in eastern Canada and eastern U.S. was 86-88% in southeastern Canada and 84-87% at one Atlantic site (KEJ) for the 2000-2018 period (Table S6). The response in total oxidized N deposition at a west coast site (SAT) to NO<sub>x</sub> emissions decrease in western Canada was 113%. The response in total oxidized deposition at the Canadian west coast site to NO<sub>x</sub> emissions reductions in the western U.S. was only 42%. Thus, both domestic and transboundary emissions reductions were pivotal in decreasing total oxidized N deposition in eastern Canada, whereas domestic emissions reductions were more effective in decreasing the deposition at the west coast site. Emissions reductions were also more effective in decreasing dry N deposition than wet oxidized N deposition. The responses in dry and wet oxidized N deposition in southeastern Canada to NO<sub>x</sub> emissions decrease were 103-106% and 85-87%, respectively (Table S6).

Unlike oxidized N, the quantitative linkage between total reduced N deposition and NH<sub>3</sub> emissions is uncertain because of missing data on long-term NH<sub>3</sub> dry deposition in this study (Table S7). The lack of trend in wet NH<sub>4</sub><sup>+</sup> deposition at Canadian rural sites was consistent with NH<sub>3</sub> emissions in eastern Canada (a slight decreasing trend) and the eastern U.S (no trend) (Fig. S5a). Increasing wet NH<sub>4</sub><sup>+</sup> deposition trends at U.S. sites were ascribed to rising NH<sub>3</sub> emissions (Du et al., 2014; Li et al., 2016). However, Tan et al. (2020) suggest that total reduced N deposition in the continental U.S. changed only by 60-80% per unit change in U.S. NH<sub>3</sub> emissions. In contrast, the response in wet NH<sub>4</sub><sup>+</sup> concentration to NH<sub>3</sub> emissions in southeastern U.K. was 130% (Fowler et al., 2005).

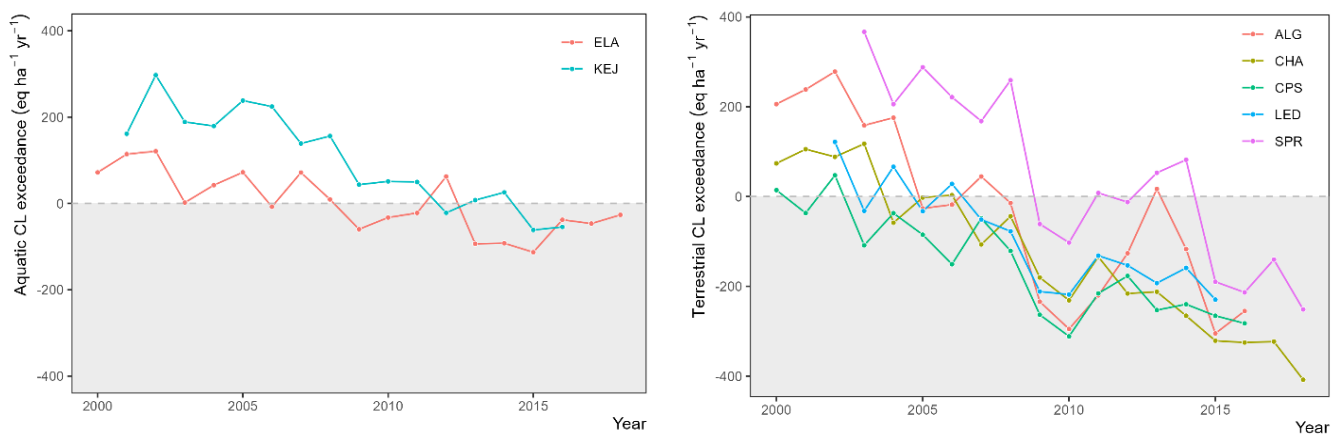
The total non-sea salt S deposition response to decreases in eastern Canadian and eastern U.S. SO<sub>2</sub> emissions was 90-96% in southeastern Canada and 108-115% in the Atlantic region (Table S8). The response in total S deposition at the west coast site to western Canadian SO<sub>2</sub> emissions reductions was 150%, whereas the response was 73% with respect to western U.S. SO<sub>2</sub> emissions reductions. The response to SO<sub>2</sub> emissions reductions were greater for dry S deposition than wet S deposition in all Canadian regions, which was also observed in the U.K. (Fowler et al., 2005) and in the eastern U.S. (Sickles and Shadwick, 2015). Thus, changes in emissions likely result in a more immediate change in dry deposition of S and oxidized N, while changes in wet deposition are less regionally coupled with emissions because of the role of meteorology.

### 3.5 Long-term trends in critical loads exceedances

Aquatic critical loads (CL) for the lakes around the five stations studied (ALG, ELA, LED, BAB and KEJ) ranged from 308 (KEJ) to 1460 eq ha<sup>-1</sup> yr<sup>-1</sup> (LED), which encompasses a large range of surface water acid-base conditions (Table S9). As expected, aquatic CL exceedances at each station showed decreasing trends with time in agreement with the decrease in total N and S deposition. Among the lakes in the five regions, the lakes of three regions (ALG, BAB and LED) showed no exceedance in any year over the 2000-2018 period because of high CL (Table S9). The selected lakes around ELA generally showed exceedance in the first half of the period but after 2008 there was no exceedance except in 2012 (Fig. 11). For the Kejimkujik (KEJ) region, the selected lakes showed high exceedances at the beginning of the period (2001-2008), whereas



exceedances were close to or below zero after 2012. The results are in good agreement with recent trends showing improved pH and alkalinity in this region although many lakes are still below critical pH and alkalinity thresholds for aquatic life (Houle et al., 2022). Indeed, the Kejimkujik region has been severely influenced by acidification of soils and surface waters and the latter are still among the most sensitive (i.e., have low base cation concentrations) and exhibit the greatest proportion 670 of acidic surface water across Canada (Jeffries et al., 2003; Houle et al., 2022). It must be noted that the lake CL estimates are based on a small number of lakes and that there may be biases in their selection (based on their proximity to the studied stations). As such, the data presented here provide a recent estimation of aquatic CL exceedances for selected lakes of five 675 regions covering a wide array of acid-base status, but this does not provide an exhaustive picture of the whole lake population at a much larger scale. Based on estimates from a previous study (Zhang et al., 2009), dry deposition of  $\text{NO}_2$ ,  $\text{NH}_3$ , PAN and unknown  $\text{NO}_y$  (non-routinely monitored species) at ALG, KEJ and LED did not result in additional years of exceedance (Table S11). Total acidic deposition exceeded CL at KEJ by an additional 8% in 2002, while it remained significantly below the CL at ALG and LED in 2003 because of the high base cation levels in the lakes.



680 **Figure 11: Aquatic (left) and terrestrial (right) critical load (CL) exceedances from 2000-2018 under total (sulfur and nitrogen) deposition for the stations experiencing exceedance at any point in the time series. The grey area represents non-exceedance. Note: stations with deposition fluxes below CL in every year from 2000-2018 are not shown.**

Terrestrial critical loads were estimated at 14 stations showing very low terrestrial  $\text{CL}_{\text{maxS}}$  at BAB ( $208 \text{ eq ha}^{-1} \text{ yr}^{-1}$ ) and 685  $\text{CL}_{\text{maxS}}$  values below  $500 \text{ eq ha}^{-1} \text{ yr}^{-1}$  for MIN, CPS, and LED (Table S10). Poor weathering rates characterized the soil CL at these four stations; these sites have shallow soils (i.e. 30 cm or less) underlain by acidic parent material. The three southern stations (LON, EGB, FRE) had the highest  $\text{CL}_{\text{maxS}}$ ; these stations are situated in areas with deeper soils (up to 50 cm) and alkaline parent material. Relatively high  $\text{CL}_{\text{maxN}}$  caused by poorly drained soils (high denitrification fraction) characterized the BON site. Five of the 14 stations received total N+S deposition in exceedance of their terrestrial CL at 690 some point in time across the study period (Fig. 11). The SPR site represented the highest initial terrestrial CL exceedance (beginning in 2003) and steepest decline into non-exceedance of the five exceeded sites; ALG followed a similar trend. The



CPS site was only briefly in exceedance during a period of high deposition in 2000 and 2002. Wet deposition was the main driver of the majority of the acidic deposition, and wet  $\text{SO}_4^{2-}$  alone resulted in terrestrial CL exceedance at these five stations. Terrestrial ecosystems in exceedance of their CL are at risk for decreased soil base saturation, mobilization of root-  
695 toxic aluminum ions, and reduced plant growth. While soils may be slower to recover from acidification, the trend into non-exceedance by the terrestrial sites is encouraging and consistent with indications that forest soils in North America are gradually recovering (Lawrence et al., 2015; Hazlett et al., 2020).

Figure 11 shows fluctuations in the exceedances with deposition just below or at the terrestrial CL at a few sites (e.g., CHA  
700 in 2004-2006 and LED in 2003/2005). The inclusion of  $\text{NO}_2$ ,  $\text{NH}_3$ , PAN and unknown  $\text{NO}_y$  dry deposition reported in our previous study (Zhang et al., 2009) resulted in CL exceedance at CHA in 2004 and near exceedance at LED in 2003 (Table S11). This suggests that the dry deposition of other N compounds cannot be neglected at sites where the difference between the CL and total deposition from routinely-monitored N is small. Even with the increased total N deposition at EGB due to  
705 the additional N flux, terrestrial CL was not in exceedance in 2002 or 2010 because of the high  $\text{CL}_{\text{maxS}}$  and  $\text{CL}_{\text{maxN}}$  at EGB (Table S10).

Exceedances of terrestrial and aquatic CL presented here are not a direct comparison with regards to area, data sources or methodology, and are presented separately to illustrate how CL exceedance responds to acidic deposition trends. Aquatic and terrestrial CL are subject to a number of uncertainties, including those in the input data (e.g. runoff, satellite land cover  
710 identification, soil data) and in the methodology (e.g. selection of a critical chemical criterion) (Hall et al., 2001). The terrestrial CL used a map-based approach that introduces additional uncertainty from the application of regional maps to local sites. The resulting CL estimates, however, have been shown to have less uncertainty than the individual model inputs because of compensating errors (Suutari et al., 2001; Skeffington et al., 2007).

#### 4 Conclusions

715 Data at 15 rural and remote CAPMoN sites were used to estimate dry and wet N and S deposition fluxes from 2000 to 2018. Acidic deposition at 14 sites decreased significantly during this period. While the declining trend in acidic deposition was modest at the west coast site, the decrease in acidic deposition was much greater in southeastern Canada. Total N deposition in southeastern Canada decreased from 6.3-11.6  $\text{kg N ha}^{-1} \text{yr}^{-1}$  during 2000-2004 to 4.0-7.9  $\text{kg N ha}^{-1} \text{yr}^{-1}$  during 2014-2018, excluding dry deposition of  $\text{NH}_3$  and some oxidized N compounds. Total S deposition for the respective periods were 5.4-  
720 12.9  $\text{kg S ha}^{-1} \text{yr}^{-1}$  and 1.8-3.8  $\text{kg S ha}^{-1} \text{yr}^{-1}$  in southeastern Canada. Our analysis showed that decreases in total S deposition were driven by reductions in wet  $\text{SO}_4^{2-}$  deposition and dry  $\text{SO}_2$  deposition, while decreases in total N deposition were largely attributed to reductions in wet and dry oxidized N deposition. Changes in total ammonium deposition were not significant.



The long-term decrease in acidic deposition can be explained by reductions in anthropogenic SO<sub>2</sub> and NO<sub>x</sub> emissions in Canada and the U.S.

725

To assess the effects of acidic deposition on Canadian ecosystems, critical loads of acidity were estimated for soils and lakes surrounding the monitoring sites. Although ecosystem damage likely occurred in acid-sensitive regions throughout the early 2000s, no significant exceedances of aquatic and terrestrial critical loads were observed after 2012 according to the SSWC and SMB steady-state CL models. It is important to emphasize that the legacy effects of acidification on ecosystems have 730 not been resolved. While the models indicate that under post-2012 deposition, the ecosystems are not exceeded, they do not indicate when the ecosystems will reach non-exceedance. The critical loads analysis presented in this paper is a case study, and there are some lakes in eastern Canada that continue to be very acidic. Moreover, the deposition sites were not selected based on their representation of acid-sensitive soils or lakes.

735

Continued monitoring and tracking of long-term trends in total S and N deposition across Canada is essential, particularly in western Canada and the prairie provinces where SO<sub>2</sub> and NO<sub>x</sub> emissions reductions are modest and NH<sub>3</sub> emissions are rising. N and S monitoring sites have been added in western Canada since 2015 to track long-term emissions and acidic deposition trends in that region. The selection of new deposition monitoring sites needs to consider high risk areas where differences 740 between acidic deposition and critical loads are marginal and where emissions of N and/or S are increasing. As oxidized N in air and in deposition continue to decrease, reduced N will comprise a larger proportion of the total N deposition at a greater number of sites. Thus, a greater focus is needed to track ammonia emissions and reduced N deposition trends and understand other drivers of variability (e.g. climate variability and changes in the atmospheric chemistry). Emerging research in Europe and the U.S point to the growing importance in acquiring a complete N deposition budget, not only for mapping critical loads of acidity but also mapping thresholds for eutrophication. Future work will also include mapping 745 continuous acidic deposition fluxes through model-measurement fusion to supplement monitoring networks and using the resulting high spatial resolution fluxes to conduct a detailed study of the impacts of acidification on Canadian ecosystems.

**Data Availability.** The data used in this publication can be accessed via the links provided in the references.

**Author Contribution.** IC analyzed the data, generated most of the figures and tables, and prepared the manuscript with 750 contributions from co-authors. LZ designed and oversaw the project with input from AC, AMM and JB. LZ and ZH generated dry deposition flux data. HC, DH and JA generated the critical loads data and wrote the corresponding sections. JF provided discussions on the air concentration and wet deposition flux for eastern Canada and the eastern U.S. JO was responsible for both measurement and data curation of 2010 continuous ambient nitrogen at the Egbert site. All coauthors have commented and/or edited the manuscript.

755 **Competing Interests.** The authors declare that they have no conflict of interest.



## Acknowledgements

This study is funded by Environment and Climate Change Canada's (ECCC) Air Pollution program. The authors acknowledge the Canadian National Atmospheric Chemistry (NAtChem) Particulate Matter and Precipitation Chemistry Databases and its data contributing agencies/organizations for the provision of data (2000-2018); ECCC's Air Pollutant Emissions Inventory and USEPA Air Emissions Inventory data used in this publication. The authors thank the CAPMoN field and lab teams including the dedicated site operators; Kulbir Banwait, Bill Sukloff, Amy Hou, Gary Yip and Greg Skelton for QA/QC and data support; Suzanne Couture for providing the Quebec and Maritimes lakes long-term average chemistry data; Michael Paterson from the International Institute for Sustainable Development-Experimental Lake Area (ELA) for providing the long-term chemistry data average of the five reference lakes in ELA as well as discharge data from lake 239.

## References

Altshuller, A., 1979. Model predictions of the rates of homogeneous oxidation of sulfur dioxide to sulfate in the troposphere. *Atmospheric Environment*, 13, 1653-1661.

Aherne, J. and Jeffries, D., 2015. Critical Load Assessments and Dynamic Model Applications for Lakes in North America. In: de Vries W., Hettelingh JP., Posch M. (eds) Critical Loads and Dynamic Risk Assessments. *Environmental Pollution*, vol 25. Springer, Dordrecht. [https://doi.org/10.1007/978-94-017-9508-1\\_19](https://doi.org/10.1007/978-94-017-9508-1_19).

Benish, S. E., Bash, J. O., Foley, K. M., Appel, K. W., Hogrefe, C., Gilliam, R., and Pouliot, G., 2022. Long-term Regional Trends of Nitrogen and Sulfur Deposition in the United States from 2002 to 2017, *Atmos. Chem. Phys. Discuss.* [preprint], <https://doi.org/10.5194/acp-2022-201>, in review.

Bergström, A. K. and Jansson, M., 2006. Atmospheric nitrogen deposition has caused nitrogen enrichment and eutrophication of lakes in the northern hemisphere. *Global Change Biology*, 12(4), 635-643.

Brakke, D. F., Henriksen, A., and Norton, S. A., 1990. A variable F-factor to explain changes in base cation concentration as a function of strong acid deposition. *Verh. Int. Verein. Limnol.*, 24, 146–149.

Brook, J. R., Samson, P. J., and Sillman, S., 1994. A meteorology-based approach to detecting the relationship between changes in SO<sub>2</sub> emission rates and precipitation concentrations of sulfate. *Journal of Applied Meteorology and Climatology*, 33(9), 1050-1066.

Burns, D. A., Bhatt, G., Linker, L. C., Bash, J. O., Capel, P. D., and Shenk, G. W., 2021. Atmospheric nitrogen deposition in the Chesapeake Bay watershed: A history of change. *Atmospheric Environment*, 251, doi: 10.1016/j.atmosenv.2021.118277.

Butler, T., Vermeylen, F., Lehmann, C. M., Likens, G. E., and Puchalski, M., 2016. Increasing ammonia concentration trends in large regions of the USA derived from the NADP/AMoN network. *Atmospheric Environment*, 146, 132-140.

Carslaw, D. C. and Ropkins, K., 2012. Openair --- an R package for air quality data analysis. *Environmental Modelling and Software*, 27-28, 52-61.



Cheng, I. and Zhang, L., 2017. Long-term air concentrations, wet deposition, and scavenging ratios of inorganic ions, HNO<sub>3</sub>, and SO<sub>2</sub> and assessment of aerosol and precipitation acidity at Canadian rural locations. *Atmospheric Chemistry and Physics*, 17(7), 4711-4730.

790 CLRTAP, 2004. Manual on Methodologies and Criteria for Modelling and Mapping Critical Loads and Levels and Air Pollution Effects, Risks and Trends. CLRTAP. [www.icpmapping.org](http://www.icpmapping.org)

Driscoll, C. T., Lawrence, G. B., Bulger, A. J., Butler, T. J., Cronan, C. S., Eagar, C., Lambert, K. F., Likens, G. E., Stoddard, J. L. and Weathers, K. C., 2001. Acidic Deposition in the Northeastern United States: Sources and Inputs, 795 Ecosystem Effects, and Management Strategies: The effects of acidic deposition in the northeastern United States include the acidification of soil and water, which stresses terrestrial and aquatic biota. *BioScience*, 51(3), pp.180-198.

Du, E., de Vries, W., Galloway, J. N., Hu, X., and Fang, J., 2014. Changes in wet nitrogen deposition in the United States between 1985 and 2012. *Environmental Research Letters*, 9(9), doi:10.1088/1748-9326/9/9/095004.

Environment and Climate Change Canada (ECCC), 2017. Canadian Air and Precipitation Monitoring Network (CAPMoN). 800 Available at: <https://open.canada.ca/data/en/dataset/4baa2ee4-a8aa-457a-af26-aa13e96ee2f4>

Environment and Climate Change Canada (ECCC), 2021a. Canada's Air Pollutant Emissions Inventory. Available at: <https://open.canada.ca/data/en/dataset/fa1c88a8-bf78-4fcb-9c1e-2a5534b92131>

Environment and Climate Change Canada (ECCC), 2021b. Major ions. Government of Canada Open Data Portal. Available at: <https://open.canada.ca/data/en/dataset/9974e51f-2616-42bf-8b40-ed12de91a304>

805 Environment and Climate Change Canada (ECCC), 2021c. Major ions and acidifying gases. Government of Canada Open Data Portal. Available at: <https://open.canada.ca/data/en/dataset/10ec2a54-9b6d-4dd7-9b05-5c30b9fa4920>

Environment and Climate Change Canada (ECCC), Meteorological Services of Canada. 2004 Canadian Acid Deposition Science Assessment. ISBN 0-662-38754-6.

Ellis, R. A., Jacob, D. J., Sulprizio, M. P., Zhang, L., Holmes, C. D., Schichtel, B. A., Blett, T., Porter, E., Pardo, L. H. and 810 Lynch, J. A., 2013. Present and future nitrogen deposition to national parks in the United States: critical load exceedances. *Atmospheric Chemistry and Physics*, 13(17), 9083-9095.

Feng, J., Chan, E., and Vet, R., 2020. Air quality in the eastern United States and Eastern Canada for 1990–2015: 25 years of change in response to emission reductions of SO<sub>2</sub> and NO<sub>x</sub> in the region. *Atmospheric Chemistry and Physics*, 20(5), 3107-3134.

815 Feng, J., Vet, R., Cole, A., Zhang, L., Cheng, I., O'Brien, J., and Macdonald, A. M., 2021. Inorganic chemical components in precipitation in the eastern US and Eastern Canada during 1989–2016: Temporal and regional trends of wet concentration and wet deposition from the NADP and CAPMoN measurements. *Atmospheric Environment*, 254, doi: 10.1016/j.atmosenv.2021.118367.

Flechard, C. R., Nemitz, E., Smith, R. I., Fowler, D., Vermeulen, A. T., Bleeker, A., Erisman, J. W., Simpson, D., Zhang, L., 820 Tang, Y. S. and Sutton, M. A., 2011. Dry deposition of reactive nitrogen to European ecosystems: a comparison of inferential models across the NitroEurope network. *Atmospheric Chemistry and Physics*, 11(6), 2703-2728.



Fowler, D., Smith, R. I., Muller, J. B. A., Hayman, G., and Vincent, K. J., 2005. Changes in the atmospheric deposition of acidifying compounds in the UK between 1986 and 2001. *Environmental Pollution*, 137(1), 15-25.

Gasset, N., Fortin, V., Dimitrijevic, M., Carrera, M., Bilodeau, B., Muncaster, R., Gaborit, E., Roy, G., Pentcheva, N., Bulat, 825 M., Wang, X., Pavlovic, R., Lespinas, F., Khedhaouiria, D., and Mai, J., 2021. A 10 km North American precipitation and land-surface reanalysis based on the GEM atmospheric model. *Hydrological and Earth System Sciences*, 25, 4917-4945.

Hall, J., Reynolds, B., Aherne, J., and Hornung, M., 2001. The importance of selecting appropriate criteria for calculating acidity critical loads for terrestrial ecosystems using the simple mass balance equation. *Water, Air and Soil Pollution*, Focus, 1(1), 29-41.

830 Hazlett, P. W., Emilson, C. E., Lawrence, G. B., Fernandez, I. J., Ouimet, R., and Bailey, S. W., 2020. Reversal of forest soil acidification in the northeastern United States and eastern Canada: Site and soil factors contributing to recovery. *Soil Systems*, 4(3), <https://doi.org/10.3390/soilsystems4030054>.

Holland, E. A., Braswell, B. H., Sulzman, J., and Lamarque, J. F., 2005. Nitrogen deposition onto the United States and Western Europe: synthesis of observations and models. *Ecological Applications*, 15(1), 38-57.

835 Houle, D., Augustin, F., and Couture, S., 2022. Rapid improvement of lake acid-base status in Atlantic Canada following steep decline in precipitation acidity. *Canadian Journal of Fisheries and Aquatic Sciences* (submitted).

Hu, C., Griffis, T. J., Frie, A., Baker, J. M., Wood, J. D., Millet, D. B., Yu, Z., Yu, X. and Czarnetzki, A. C., 2021. A multiyear constraint on ammonia emissions and deposition within the US corn belt. *Geophysical Research Letters*, 48(6), e2020GL090865, <https://doi.org/10.1029/2020GL090865>.

840 Jeffries, D. S., Clair, T. A., Couture, S., Dillon, P. J., Dupont, J., Keller, W., McNicol, D. K., Turner, M. A., Vet, R., Weeber, R., 2003. Assessing the Recovery of Lakes in Southeastern Canada from the Effects of Acidic Deposition. *AMBIO: A Journal of the Human Environment*, 32, (3), 176-182.

Jeffries, D. S., Semkin, R. G., Gibson, J. J., and Wong, I., 2010. Recently surveyed lakes in northern Manitoba and Saskatchewan, Canada: characteristics and critical loads of acidity. *Journal of Limnology*, 69, 45-55.

845 Kharol, S. K., Shephard, M. W., McLinden, C. A., Zhang, L., Sioris, C. E., O'Brien, J. M., Vet, R., Cady-Pereira, K. E., Hare, E., Siemons, J. and Krotkov, N. A., 2018. Dry deposition of reactive nitrogen from satellite observations of ammonia and nitrogen dioxide over North America. *Geophysical Research Letters*, 45(2), 1157-1166.

Lawrence, G. B., Hazlett, P. W., Fernandez, I. J., Ouimet, R., Bailey, S. W., Shortle, W. C., Smith, K. T., and Antidormi, M. R., 2015. Declining Acidic Deposition Begins Reversal of Forest-Soil Acidification in the Northeastern U.S. and Eastern 850 Canada. *Environmental Science and Technology*, 49(22), 13103-13111.

Lee, C., Martin, R. V., van Donkelaar, A., Lee, H., Dickerson, R. R., Hains, J. C., Krotkov, N., Richter, A., Vinnikov, K. and Schwab, J.J., 2011. SO<sub>2</sub> emissions and lifetimes: Estimates from inverse modeling using in situ and global, space-based (SCIAMACHY and OMI) observations. *Journal of Geophysical Research: Atmospheres*, 116(D06304), doi:10.1029/2010JD014758.



855 Lehmann, C. M., Bowersox, V. C., Larson, R. S., and Larson, S. M., 2007. Monitoring long-term trends in sulfate and ammonium in US precipitation: Results from the National Atmospheric Deposition Program/National Trends Network. *Water Air and Soil Pollution, Focus*, 7, 59-66, doi: 10.1007/s11267-006-9100-z.

Li, Y., Schichtel, B. A., Walker, J. T., Schwede, D. B., Chen, X., Lehmann, C. M., Puchalski, M. A., Gay, D. A. and Collett, J. L., 2016. Increasing importance of deposition of reduced nitrogen in the United States. *Proceedings of the National Academy of Sciences*, 113(21), 5874-5879.

860 Likens, G. E., Butler, T. J., Claybrooke, R., Vermeylen, F., and Larson, R., 2021. Long-term monitoring of precipitation chemistry in the US: Insights into changes and condition. *Atmospheric Environment*, 245, doi: 10.1016/j.atmosenv.2020.118031.

Liu, X., Zhang, Y., Han, W., Tang, A., Shen, J., Cui, Z., Vitousek, P., Erisman, J. W., Goulding, K., Christie, P., Fangmeier, A., and Zhang, F., 2013. Enhanced nitrogen deposition over China. *Nature*, 494(7438), 459-462.

865 Makar, P. A., Akingunola, A., Aherne, J., Cole, A. S., Aklilu, Y.-A., Zhang, J., Wong, I., Hayden, K., Li, S.-M., Kirk, J., Scott, K., Moran, M. D., Robichaud, A., Cathcart, H., Baratzedah, P., Pabla, B., Cheung, P., Zheng, Q., and Jeffries, D. S., 2018. Estimates of exceedances of critical loads for acidifying deposition in Alberta and Saskatchewan. *Atmospheric Chemistry and Physics*, 18, 9897-9927.

870 McHale, M. R., Ludtke, A. S., Wetherbee, G. A., Burns, D. A., Nilles, M. A., and Finkelstein, J. S., 2021. Trends in precipitation chemistry across the US 1985–2017: Quantifying the benefits from 30 years of Clean Air Act amendment regulation. *Atmospheric Environment*, 247, 118219.

McMillan, A. C., MacIver, D., and Sukloff, W. B., 2000. Atmospheric environmental information – an overview with Canadian examples. *Environmental Modelling and Software*, 15, 245–248.

875 Moran, M. D., Lupu, A., Zhang, J., Savic-Jovcic, V., and Gravel, S., 2018. A Comprehensive Performance Evaluation of the Next Generation of the Canadian Operational Regional Air Quality Deterministic Prediction System. In C. Mensink & G. Kallos (Eds.), *Air Pollution Modeling and its Application XXV* (pp. 75–81). Springer International Publishing. [https://doi.org/10.1007/978-3-319-57645-9\\_12](https://doi.org/10.1007/978-3-319-57645-9_12)

Nilsson, J. and Grennfelt, P., 1988. Critical loads for sulphur and nitrogen. Report from a workshop held at Skokloster, 880 Sweden. Miljørapport 1988:15, Nordic Council of Ministers, Copenhagen, Denmark. 31 pp.

Nopmongcol, U., Beardsley, R., Kumar, N., Knipping, E., and Yarwood, G., 2019. Changes in United States deposition of nitrogen and sulfur compounds over five decades from 1970 to 2020. *Atmospheric Environment*, 209, 144-151.

Pan, Y. P., Wang, Y. S., Tang, G. Q., and Wu, D., 2012. Wet and dry deposition of atmospheric nitrogen at ten sites in Northern China. *Atmospheric Chemistry and Physics*, 12(14), 6515-6535.

885 Pan, D., Benedict, K.B., Golston, L.M., Wang, R., Collett, J. L., Tao, L., Sun, K., Guo, X., Ham, J., Prenni, A. J., Schichtel, B.A., Mikoviny, T., Muller, M., Wisthaler, A., and Zondlo, M. A., 2021. Ammonia Dry Deposition in an Alpine Ecosystem Traced to Agricultural Emission Hotspots. *Environmental Science and Technology*, 55(12), 7776-7785.



Pardo, L. H., Fenn, M. E., Goodale, C. L., Geiser, L. H., Driscoll, C. T., Allen, E. B., Baron, J. S., Bobbink, R., Bowman, W. D., Clark, C. M., Emmett, B., Gilliam, F. S., Greaver, T. L., Hall, S. J., Lilleskov, E. A., Liu, L., Lynch, J. A., Nadelhoffer, 890 K. J., Perakis, S. S., Robin-Abbott, M. J., Stoddard, J. L., Weathers, K. C., and Dennis, R. L., 2011. Effects of nitrogen deposition and empirical nitrogen critical loads for ecoregions of the United States. *Ecological Applications*, 21(8), 3049-3082.

Posch, M., de Vries, W., and Sverdrup, H. U., 2015. Mass Balance Models to Derive Critical Loads of Nitrogen and Acidity for Terrestrial and Aquatic Ecosystems. In W. de Vries, J.-P. Hettelingh, & M. Posch (Eds.), *Critical Loads and Dynamic Risk Assessments: Nitrogen, Acidity and Metals in Terrestrial and Aquatic Ecosystems* (pp. 171–205). Springer Netherlands. [https://doi.org/10.1007/978-94-017-9508-1\\_6](https://doi.org/10.1007/978-94-017-9508-1_6)

Posch, M., Kämäri, J., Johansson, M., and Forsius, M., 1993. Displaying inter-and intra-regional variability of large-scale survey results. *Environmetrics*, 4(3), 341–352.

Sirois, A. and Fricke, W., 1992. Regionally representative daily air concentrations of acid-related substances in Canada; 1983–1987. *Atmospheric Environment*, 26(4), 593-607.

900 Sirois, A., Vet, R., and Lamb, D., 2000. A comparison of the precipitation chemistry measurements obtained by the CAPMoN and NADP/NTN networks. *Environmental Monitoring and Assessment*, 62(3), 273-303.

Schwede, D., Zhang, L., Vet, R., and Lear, G., 2011. An intercomparison of the deposition models used in the CASTNET and CAPMoN networks. *Atmospheric Environment*, 45(6), 1337-1346.

Shao, S., Driscoll, C. T., Sullivan, T. J., Burns, D. A., Baldigo, B., Lawrence, G. B., and McDonnell, T. C., 2020. The 905 response of stream ecosystems in the Adirondack region of New York to historical and future changes in atmospheric deposition of sulfur and nitrogen. *Science of the Total Environment*, 716, doi: 10.1016/j.scitotenv.2020.137113.

Sickles II, J. E. and Shadwick, D. S., 2015. Air quality and atmospheric deposition in the eastern US: 20 years of change. *Atmospheric Chemistry and Physics*, 15(1), 173-197.

Skeffington, R.A., Hall, J.R., Heywood, E., Wadsworth, R.A., Whitehead, P., Reynolds, B., Abbott, J. and Vincent, K., 910 2007. *Uncertainty in critical load assessment models*. Science Report: SC030172/SR. Technical Report. Environment Agency, Bristol.

Suutari, R., Amann, M., Cofala, J., Klimont, Z., Posch, M., and Schöpp, W., 2001. From economic activities to ecosystem protection in Europe: An uncertainty analysis of two scenarios of the RAINS integrated assessment model. CIAM/CCE Rep. 1/2001.

915 Staelens, J., Wuyts, K., Adriaenssens, S., Van Avermaet, P., Buysse, H., Van den Bril, B., Roekens, E., Ottoy, J.P., Verheyen, K., Thas, O. and Deschepper, E., 2012. Trends in atmospheric nitrogen and sulphur deposition in northern Belgium. *Atmospheric Environment*, 49, 186-196.

Sverdrup, H., 1990. *The kinetics of base cation release due to chemical weathering*. Krieger Publishing Company.

Sverdrup, H. and De Vries, W., 1994. Calculating critical loads for acidity with the simple mass balance method. *Water, Air, 920 and Soil Pollution*, 72(1), 143–162. <https://doi.org/10.1007/BF0125712>.



Tan, J., Fu, J. S., and Seinfeld, J. H., 2020. Ammonia emission abatement does not fully control reduced forms of nitrogen deposition. *Proceedings of the National Academy of Sciences*, 117(18), 9771-9775.

USEPA, 2021. Air pollutant emissions trends data. Available at: <https://www.epa.gov/air-emissions-inventories/air-pollutant-emissions-trends-data>

925 Vet, R., Artz, R. S., Carou, S., Shaw, M., Ro, C. U., Aas, W., Baker, A., Bowersox, V. C., Dentener, F., Galy-Lacaux, C., Hou, A., Pienaar, J. J., Gillett, R., Forti, M. C., Gromov, S., Hara, H., Khodzher, T., Mahowald, N. M., Nickovic, S., Rao, P. S. P., and Reid, N. W., 2014. A global assessment of precipitation chemistry and deposition of sulfur, nitrogen, sea salt, base cations, organic acids, acidity and pH, and phosphorus. *Atmospheric Environment*, 93, 3-100.

Walker, J. T., Beachley, G., Zhang, L., Benedict, K. B., Sive, B. C., and Schwede, D. B., 2020. A review of measurements of 930 air-surface exchange of reactive nitrogen in natural ecosystems across North America. *Science of The Total Environment*, 698, 133975.

Walker, J. T., Beachley, G., Amos, H. M., Baron, J. S., Bash, J., Baumgardner, R., Bell, M. D., Benedict, K. B., Chen, X., Clow, D. W., Cole, A., Coughlin, J. G., Cruz, K., Daly, R. W., Decina, S. M., Elliott, E. M., Fenn, M. E., Ganzeveld, L., Gebhart, K., Isil, S. S., Kerschner, B. M., Larson, R. S., Lavery, T., Lear, G. G., Macy, T., Mast, M. A., Mishoe, K., Morris, 935 Padgett, P. E., Pouyat, R. V., Puchalski, M., Pye, H., Rea, A. W., Rhodes, M. F., Rogers, C. M., Saylor, R., Scheffe, R., Schichtel, B. A., Schwede, D. B., Sexstone, G. A., Sive, B. C., Sosa, R., Templer, P. H., Thompson, T., Tong, D., Wetherbee, G. A., Whitlow, T. H., Wu, Z., Yu, Z., and Zhang, L., 2019. Toward the improvement of total nitrogen deposition budgets in the United States. *Science of The Total Environment*, 691, 1328–1352.

Wen, Z., Xu, W., Li, Q., Han, M., Tang, A., Zhang, Y., Luo, X., Shen, J., Wang, W., Li, K., Pan, Y., Zhang, L., Li, W., 940 Collett, J. R., Zhong, B., Wang, X., Goulding, K., Zhang, F., and Liu, X., 2020. Changes of nitrogen deposition in China from 1980 to 2018. *Environment International*, 144, 106022, <https://doi.org/10.1016/j.envint.2020.106022>.

World Meteorological Organization (WMO) Global Atmosphere Watch, 2004. Manual for the GAW Precipitation Chemistry Programme, Guidelines Data Quality Objectives and Standard Operating Procedures. No. 160.

Wright L. P., Zhang L., Cheng I., Aherne J., and Wentworth G. R., 2018. Impacts and effects indicators of atmospheric 945 deposition of major pollutants to various ecosystems – A review. *Aerosol and Air Quality Research*, 18, 1953-1992.

Xu, W., Luo, X. S., Pan, Y. P., Zhang, L., Tang, A. H., Shen, J. L., Zhang, Y., Li, K. H., Wu, Q. H., Yang, D. W., Zhang, Y. Y., Xue, J., Li, W. Q., Li, Q. Q., Tang, L., Lu, S. H., Liang, T., Tong, Y. A., Liu, P., Zhang, Q., Xiong, Z. Q., Shi, X. J., Wu, L. H., Shi, W. Q., Tian, K., Zhong, X. H., Shi, K., Tang, Q. Y., Zhang, L. J., Huang, J. L., He, C. E., Kuang, F. H., Zhu, B., Liu, H., Jin, X., Xin, Y. J., Shi, X. K., Du, E. Z., Dore, A. J., Tang, S., Collett Jr., J. L., Goulding, K., Sun, Y. X., Ren, J., 950 Zhang, F. S., and Liu, X. J., 2015. Quantifying atmospheric nitrogen deposition through a nationwide monitoring network across China. *Atmospheric Chemistry and Physics*, 15, 12345–12360.

Yao, X. and Zhang, L., 2016. Trends in atmospheric ammonia at urban, rural and remote sites across North America. *Atmospheric Chemistry and Physics*, 16, 11465-11475.



955 Yu, G., Jia, Y., He, N., Zhu, J., Chen, Z., Wang, Q., Piao, S., Liu, X., He, H., Guo, X., Wen, Z., Li, P., Ding, G., and  
Goulding, K., 2019. Stabilization of atmospheric nitrogen deposition in China over the past decade. *Nature Geoscience*, 12,  
424-429.

Zbieranowski, A. L. and Aherne, J., 2011. Long-term trends in atmospheric reactive nitrogen across Canada: 1988–2007.  
*Atmospheric Environment*, 45(32), 5853-5862.

960 Zhang, L. and He, Z., 2014. Technical note: An empirical algorithm estimating dry deposition velocity of fine, coarse and  
giant particles. *Atmospheric Chemistry and Physics*, 14(7), 3729-3737.

Zhang, L., Brook, J. R., and Vet, R., 2003. A revised parameterization for gaseous dry deposition in air-quality models.  
*Atmospheric Chemistry and Physics*, 3(6), 2067-2082.

Zhang, L., Vet, R., O'Brien, J. M., Mihele, C., Liang, Z., and Wiebe, A., 2009. Dry deposition of individual nitrogen species  
at eight Canadian rural sites. *Journal of Geophysical Research: Atmospheres*, 114, D02301, doi:10.1029/2008JD010640.

965 Zhang, L., Vet, R., Wiebe, A., Mihele, C., Sukloff, B., Chan, E., Moran, M. D., and Iqbal, S., 2008. Characterization of the  
size-segregated water-soluble inorganic ions at eight Canadian rural sites. *Atmospheric Chemistry and Physics*, 8(23), 7133-  
7151.

Zhang, L., He, Z., Wu, Z., Macdonald, A. M., Brook, J. R., and Kharol, S., 2022. A database of modeled gridded dry  
deposition velocities for 45 gaseous species and three particle size ranges across North America. *Journal of Environmental  
970 Sciences*, in press.

Zhang, Y., Mathur, R., Bash, J. O., Hogrefe, C., Xing, J., and Roselle, S. J., 2018. Long-term trends in total inorganic  
nitrogen and sulfur deposition in the US from 1990 to 2010. *Atmospheric Chemistry and Physics*, 18(12), 9091-9106.

Zhao, Y., Zhang, L., Chen, Y., Liu, X., Xu, W., Pan, Y., and Duan, L., 2017. Atmospheric nitrogen deposition to China: A  
model analysis on nitrogen budget and critical load exceedance. *Atmospheric Environment*, 153, 32-40.